



Conference
Sports Physics 2021

ENS de Lyon

6-8 December 2021

BOOK OF ABSTRACTS



Sports Physics 2021

ENS de Lyon, 6-8 December 2021

Contents

1 Keynote 1: Riding faster thanks to research programs	
Monday 6 December - 10h50	4
2 Session 1: Sensors	
Monday 6 December - 11h50	5
2.1 Football shoes measuring on-field ground reaction forces	5
2.2 Development of a power meter for athletic wheelchair	6
2.3 Characterization of a diving board model using motion capture data	7
3 Session 2: Tribute to Lionel Manin	
Monday 6 December - 14h00	8
3.1 Preliminary modelling of roller chain drive power losses. Application to track cycling	8
3.2 Dynamical buckling of a table-tennis ball impinging normally on a rigid target: experimental and numerical studies	9
4 Session 3: Strategies	
Monday 6 December - 15h10	10
4.1 Gunwale bobbing and optimal stroke frequencies	10
4.2 Physics of kayak races	11
4.3 Exploring biomechanical strategies through optimal control in trampoline	12
4.4 Assessment of Different Underwater Undulatory Swimming (UUS) Strategies using a Two-Dimensional CFD Method	13
4.5 Rowing Race Strategy : find the optimum through hydrodynamics, biomechanics and physiology constraints.	14
5 Keynote 2: Running at Altitude: the 100-metre Dash	
Monday 6 December - 17h00	15
6 Keynote 3: Functional Electrical Stimulation Cycling: an Electrifying Sport	
Tuesday 7 December - 9h00	16
7 Session 4: Fluid dynamics 1	
Tuesday 7 December - 10h00	17
7.1 Numerical study of the influence of the spectrum of a turbulent wind on arrow trajectories	17
7.2 Wave drag in unsteady motion	18
7.3 Cycling aerodynamics	19
7.4 Cycling in the wind	20
7.5 Shaping your hand for more efficient swimming	21
8 Session 5: Energy	
Tuesday 7 December - 11h50	22
8.1 Optimal Individual Pushing Position in Rugby Scrum	22
8.2 Energies and forces during pole vault flight	23
8.3 Looking for optimal biomechanical configurations in weightlifting and powerlifting	24
8.4 Bike tire rolling resistance	25

9 Session 6: Fluid dynamics 2	
Tuesday 7 December - 14h00	26
9.1 Velocity–Stroke rate in paddle sports	26
9.2 Getting a boost from shallow water	27
9.3 Optimal swimming start	28
9.4 Drafting effect in cycling, a field study	29
9.5 Drafting of two swimmers	30
10 Session 7: Tracking/data analysis	
Tuesday 7 December - 15h50	31
10.1 Automatic detection of stroke phases in front crawl with the use of Dynamic Time Warping (DTW)	31
10.2 Geometric discrepancies in Olympic windsurf foils: measurements versus athletes' feedback	32
10.3 Prediction of wind fields using weather pattern recognition: analysis of sailing strategy and real weather data in Tokyo 2020 Olympics	33
10.4 An investigation on transfer in motor skill acquisition with machine learning.	34
11 Keynote 4: The hydrodynamics of propulsion in rowing	
Tuesday 7 December - 17h00	35
12 Keynote 5: Understanding the runner-shoe couple mechanics to prevent running-related injuries	
Wednesday 8 December - 9h00	36
13 Session 8: Interaction fluid/surface	
Wednesday 8 December - 10h00	37
13.1 Supercavitating hydrofoil for the World Sailing Speed Record	37
13.2 The aerodynamic properties of new and worn tennis balls	38
13.3 Dynamics of confined cavitation bubbles, a possible link with mild traumatic brain injuries.	39
13.4 How Ball Wear Affects Ball Aerodynamics: Do Past Methods Provide an Accurate Representation?	40
14 Session 9: Biomechanics	
Wednesday 8 December - 11h30	41
14.1 Sensitivity of scapulothoracic angle estimates to kinematic model parameters during ball throwing	41
14.2 Protocol for the mechanical characterisation of a tibial prosthesis: sensitivity study	42
14.3 Force production capacities in sprint running: Citius or Fortius ?	43
14.4 Flexibility of the motor behaviour in swimming	44
14.5 Theoretical framework of a force-velocity-endurance relation	45
15 Session 10: Material	
Wednesday 8 December - 14h00	46
15.1 Guiding blind people with spatialized sound for sport practice	46
15.2 Optimizing shoe midsoles for running performance	47
15.3 Modeling of additive manufactured lattice structures designed for shock-absorbing sports components	48
16 Keynote 6: Two short stories about data and sports	
Wednesday 8 December - 14h50	49
Alphabetical index of authors	50
Acknowledgements	51

1 **Keynote 1: Riding faster thanks to research programs**

Monday 6 December - 10h50

Brunet Emmanuel

French Cycling Federation

e.brunet@ffc.fr

Cycling and rowing federations have joined forces with several "grandes écoles" and universities to create the THPCA2024 research program. This program aims to optimize performance in these two sports for the Paris 2024 Olympic Games. Regarding cycling, there is an average increase in performance of around 1.5% every olympics. Which factors can staffs and cyclists activate in order to continue this progress ? The presentation aims to identify several factors, whether human or material, allowing to contribute to this progression of performances and give some guidelines for research on high performance in cycling.

2 Session 1: Sensors

Monday 6 December - 11h50

2.1 Football shoes measuring on-field ground reaction forces

Karamanoukian A.^{1,2,3}, Boucher J.P.³, **Labbé Romain**³ & Vignais N.^{1,2}

¹Université Paris-Saclay CIAMS, 91405, Orsay, France, ²Université d'Orléans, CIAMS, 45067, Orléans, France, ³Phyling, Palaiseau, France

alexandre.karamanoukian@universite-paris-saclay.fr

Studying ground reaction forces (GRFs) in football is key to prevent non-contact lower limb injuries caused by fatigue and excessive training load. However, the use of force plates on the field is not feasible and inertial measurement unit (IMUs) estimations have shown poor or limited validity during team sport activities or football-specific tasks [1]. Thus, the lack of portable device allowing to measure GRFs in ecological conditions currently limit the efficiency of injury-prevention programs.

The purpose of this study was to assess the validity of a football shoe fitted with 6 instrumented studs to measure GRFs on a football turf. To this aim, data collected during sprints and counter-movement jumps (CMJs) have been compared to data obtained with force platforms, i.e. the reference tool to measure GRFs. Obtained force patterns and their evolution with running velocity were in accordance with the literature [2].

This innovative way to measure GRFs could give new insights to quantify training load, detect stride imbalances and neuromuscular fatigue and have a better understanding of the player/shoe/surface interface. This instrumented football shoe could also give information about force distribution under the foot (medial vs lateral, CoP trajectories, etc.).

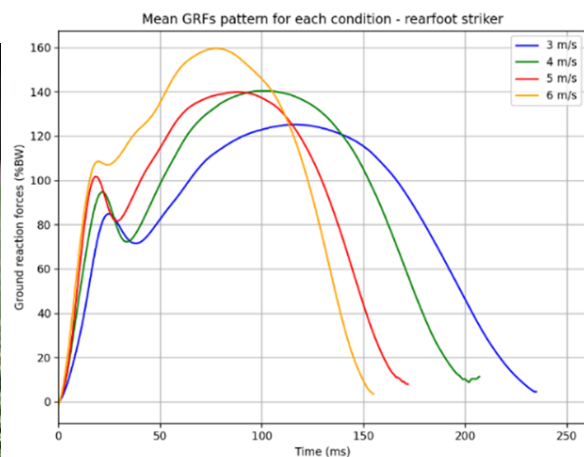


Figure 1: (a) Portable instrumented shoe prototype. (b) Mean force patterns for each velocity for a given subject.

References

- [1] Jennings, D., Cormack, S., Coutts, A. J., Boyd, L., & Aughey, R. J., *Int. J. of Sports Physio. and Perf.*, **5**, 328–341 (2010).
- [2] Hamill, J., Bates, B. T., Knutzen, K. M., & Sawhill, J. A., *Human Movement Science*, **2(1–2)**, 47–56 (1983).

2.2 Development of a power meter for athletic wheelchair

Mille Antoine & Géminard J.C.

ENS Lyon, Laboratoire de Physique

antoine.mille@ens-lyon.fr

In support to the 2024 Paralympic Games, the “Paraperf” project was selected by the Priority Research Program “Very High Performance Sport” of the National Research Agency. The project is coordinated by INSEP and brings together 14 partners in collaboration with the French Handisport Federation. “Paraperf” is an opportunity for sports sciences to invest in the field of Paralympic sport on a scale and in an unprecedented way for developing tools and methods to maximize the chances of a podium at the Paris Games.

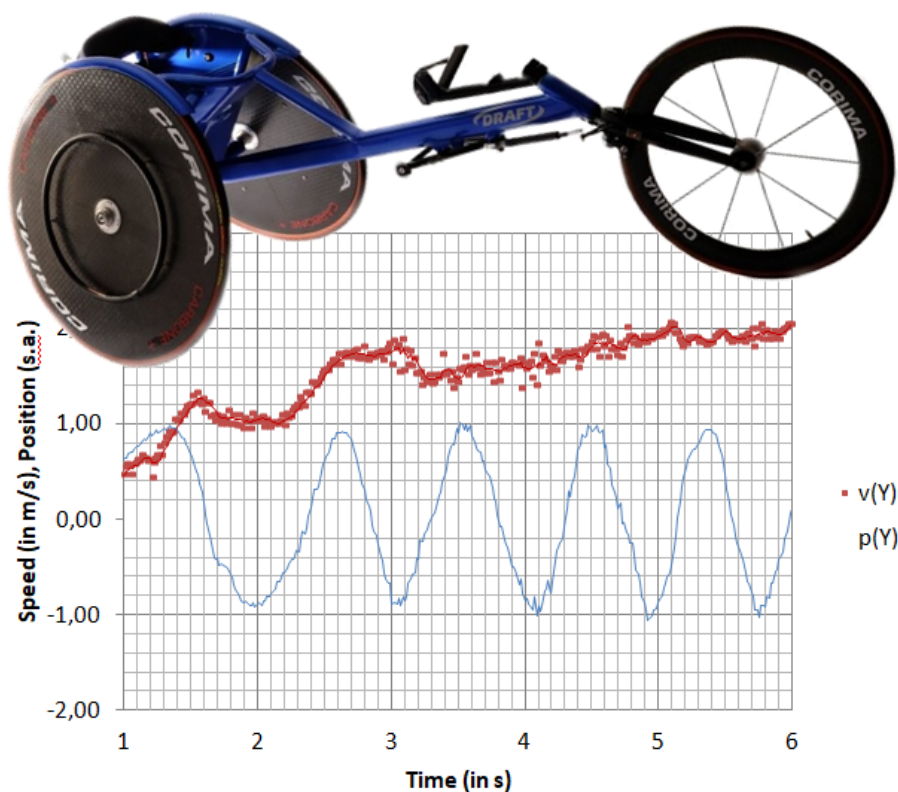


Figure 2: *Speed and angular position of a wheel as functions of time.*

In this context, the objective of our contribution at ENS Lyon is to optimize wheelchair athletes’ performance. To do so, it has been set that the monitoring of the instantaneous power developed by the competitors was relevant to optimize and rectify gesture, pace and intensity of their efforts. Thus, our goal is to design, develop and then use a pair of fully dedicated instrumented wheels which would be adaptable to any athletic wheelchair.

To begin with, the project consists of designing and mounting wheels using IMU and strain gauges in order to capture speed, angular position and the instantaneous power developed. Afterwards, the system will be connected to athlete and coach’s phone and computer to allow them to use it by themselves and adapt training and preparation to their performances and objectives.

2.3 Characterization of a diving board model using motion capture data

Demestre Louise, Grange S., Bideau N., Nicolas. G., Pontonnier C. & Dumont G.

Univ Rennes, Inria, CNRS, IRISA; Univ Lyon, INSA-Lyon, GEOMAS, Villeurbanne; Univ Rennes, Inria, Laboratoire M2S, Rennes

louise.demestre@ens-rennes.fr

Springboard diving performance is the result of the interaction between a diver and a diving board. An accurate modelling of this interaction could provide new tools to better understand how to improve diving board performance.

This study presents a finite element model of a springboard [1]. The aim is to identify the springboard parameters allowing to obtain a model with a mechanical behaviour similar to that observed experimentally. The characterization method is based on motion capture data of the diver and the diving board (4 trials involving 2 dives with a running approach and 2 dives with a starting position at the diving board free end). Firstly, these experimental data are used to estimate the interaction forces and moments (IF&M) between the diver and the diving board using an optimization approach [2]. The IF&M are then applied to the springboard model to be characterized (figure 3). Finally, the model parameters are identified minimizing the discrepancy between the experimental and numerical vertical displacements of the springboard with the simulated annealing method.

For the diving trials meeting the assumption of a diving board with a zero initial speed, a model with a maximal absolute error between the experimental and numerical vertical displacements of 0.03 m is obtained. This model may help to better understand energy transfers and time synchronisation between the diver and the diving board, which are key points of the springboard diving performance.

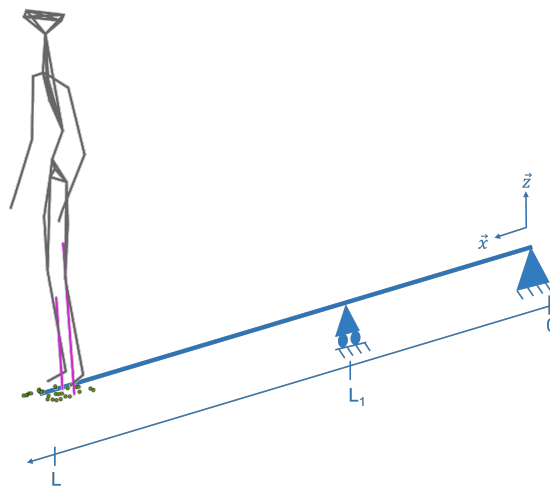


Figure 3: *Diver (IF&M for each foot in purple and contact points under the diver's feet in green) and diving board (in blue) models.*

References

- [1] Grange S., ATL4S—A Tool and Language for Simplified Structural Solution Strategy. Located at: GEOMAS INSA-Lyon, Villeurbanne, France
- [2] Muller A., Pontonnier C. & Dumont G., Motion-based prediction of hands and feet contact efforts during asymmetric handling tasks, *IEEE T Bio-Med Eng.* **67(2)**, 344-352 (2020)

3 Session 2: Tribute to Lionel Manin

Monday 6 December - 14h00

3.1 Preliminary modelling of roller chain drive power losses. Application to track cycling

Lanaspeze Gabriel, Best M., Cavoret J., Guilbert B., Manin L. & Ville F.

Univ Lyon, INSA Lyon, CNRS, LaMCoS, UMR5259, 69621 Villeurbanne, France

gabriel.lanaspeze@insa-lyon.fr

Chain drives are used since their invention, by Hans Renold, in the late 19th century. These transmissions can be found in various mechanisms, from car internal combustion engine distribution to bicycle. In track cycling, victory in top level races can be decided by milliseconds. In this context, every part of the athlete's bicycle must be optimised.

In order to study the chain drives efficiency, it is important to know what the main power loss mechanisms are and what are their relative magnitude. In this study, two sources of power loss were considered, both related to friction between chain components during transmission's motion. The first one is the meshing loss, linked to the rotational movement experienced by the chain link captured or released by one of the sprockets. The second source of loss is due to the movement of each roller along its corresponding tooth profile (Figure 4).

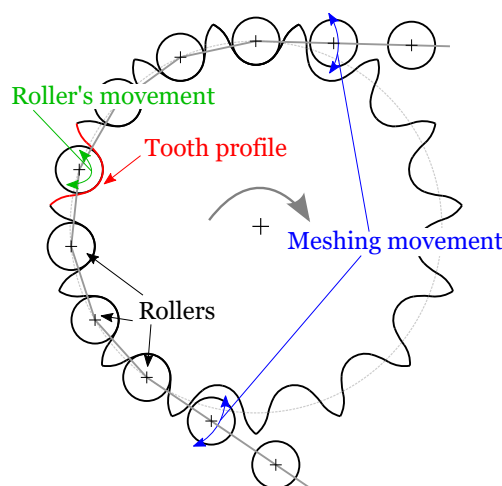


Figure 4: Sprocket with power loss sources.

To study the influence of each power loss source, it is necessary to calculate the magnitude of the forces involved in the drive and to know the relative motion of each part in contact. These quantities are evaluated using the works of Lodge [1] and Kim [2]. The estimation of each loss source allows to represent their relative influence on the overall transmission losses. It is shown that, for a typical track cycling transmission, the two sources of loss have equivalent influence.

References

- [1] C. J. Lodge and S. C. Burgess. A model of the tension and transmission efficiency of a bush roller chain. *Proceedings of the Institution of Mechanical Engineers, Part C: Journal of Mechanical Engineering Science*, 216(4):385–394, 2002.
- [2] Mahn Shik Kim and Glen E. Johnson. Mechanics of roller chain-sprocket contact: a general modelling strategy. In *American Society of Mechanical Engineers, Design Engineering Division (Publication) DE*, volume 43 pt 2, pages 689–695, 1992.

3.2 Dynamical buckling of a table-tennis ball impinging normally on a rigid target: experimental and numerical studies

Rémond Théophile, Dolique V. & Géminard J.-C.

Laboratoire de physique, ENS de Lyon/CNRS, Lyon, France.

theophile.remond@ens-lyon.f

Antony S. & Manin L.

Laboratoire de Mécanique des Contacts et des Structures, INSA Lyon/CNRS, Lyon, France.

Rinaldi R.

Laboratoire Matériaux : Ingénierie et Science, INSA Lyon/CNRS, Lyon, France.

The table tennis racket (or paddle) is a subtle assembly of layers of wood and polymeric materials (solid foam and rubber sheet). The choice of the components, which is empirical and results from the experience of the providers and users, alters drastically the characteristics of the rebound of the ball and the ability of the player to give speed and effect to the ball. This project aims to assess and understand the role played by each of the parameters having an impact on the rebound (Ball, material, geometrical characteristics,...).

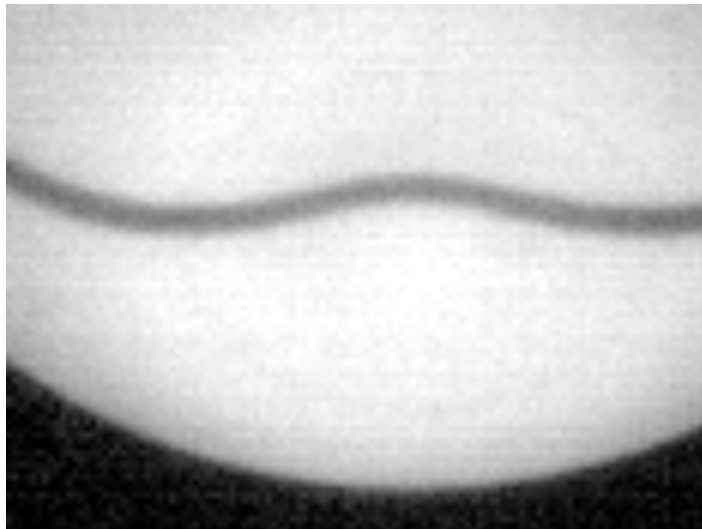


Figure 5: *Snapshot of the ball profile during the impact with the solid substrate.*

A ball impacting a rigid surface in normal incidence shows a dynamical buckling of the spherical shell. The dynamics of this phenomenon is studied. In particular, the ball buckles at a deflection of about twice the shell thickness. In addition a drop of the coefficient of restitution is observed in this range which is related to the friction in between the moving shell and the contact surface.

4 Session 3: Strategies

Monday 6 December - 15h10

4.1 Gunwale bobbing and optimal stroke frequencies

Benham Graham P.¹, Devauchelle O.², Morris S.³ & Neufeld J.A.¹

¹University of Cambridge. ²Institut de Physique du Globe de Paris. ³University of Toronto.

gpb35@cam.ac.uk

In rowing and canoe races, significant downward thrust is generated from the heaving motion of the athletes' bodies during each stroke. However, it is unknown how this force affects interactions with the wave-field of the boat, and whether this has an overall positive or negative contribution to efficiency.

The forward thrust generated by vertical heaving motion can be isolated and studied by removal of the oars/paddle, and achieving forward motion through vertical forcing only, in a manner similar to surfing one's own wave field. In this procedure, known as *Gunwale bobbing*, the boat can achieve a cruising velocity which satisfies a balance between the thrust generated from pushing downwards into the surface gradients of the wave-field and the resistance due to a combination of skin, form and wave drag.

This summer, we demonstrated the parameters for successful Gunwale bobbing in a lake using a 4 metre canoe equipped with an accelerometer [1]. A simple theoretical description, based on the linear theories of Havelock [2] and Helmholtz (for bouncing droplets) [3], explains these results and shows close comparison with optimal bobbing frequencies. Finally, we discuss perspectives from this work, including how these parameters compare to stroke frequency data from the Olympics.



Figure 6: *Sebastian Brendel of Germany competes during the Men's Canoe Single 1000m Final A, Rio de Janeiro, 2016. (Image from olympics.com).*

References

- [1] Benham G.P., Devauchelle O., Morris S. & Neufeld J.A., *in prep.* (2021)
- [2] Havelock T., Proc. R. Soc. Lond. A, **95**, 354 (1919)
- [3] Devauchelle O., Lajeunesse É., James F., Josserand C., & Lagrée P., Comptes Rendus Mécanique **348**, 591 (2020)

4.2 Physics of kayak races

Boucher Jean-Philippe¹, Prétot C.¹, Carmigniani R.², Hasbroucq L.¹, Labbé R.³ & Clanet C.¹

¹Ecole Polytechnique, ²ENPC, ³Phyling

clanet@ladhyx.polytechnique.fr

In a kayak, the paddler is seated in the direction of motion and uses a double-bladed paddle as presented in figure 7.a. Kayak races are ruled by the International Canoe Federation [1] which state that two different disciplines exist at the summer Olympics: slalom in river and sprint on flatwater which are the ones we consider.

We first study experimentally the standing start dynamics and the velocity-cadence relationship with two national level athletes (figure 7.b). We then develop a theoretical model which extends the seminal work of Jackson [2] and which captures the main features of these measurements. Finally, we use this theoretical model to develop a general optimisation race algorithm and use it to account for data collected in world championships.

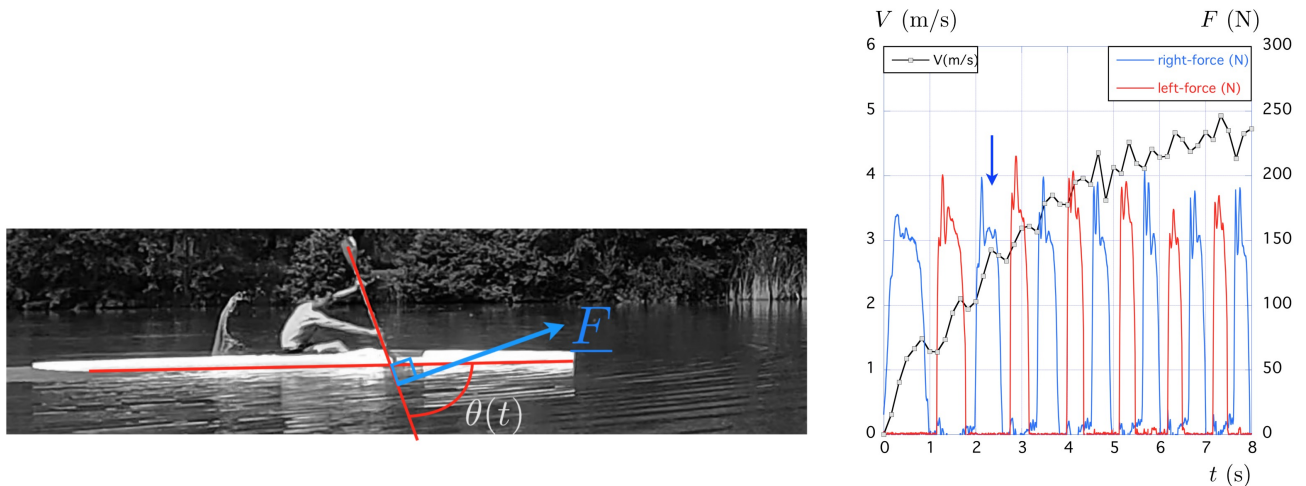


Figure 7: (a) Kayak in propulsion phase (b) Time evolution of velocity and forces during a standing start.

References

- [1] B. Berglund and D. McKenzie, Handbook of Sports Medicine and Science, Canoeing, Handbook of Sports Medicine and Science, Canoeing (2018)
- [2] P.S. Jackson, J Sports Sci. **13**, 239-45 (1995)

4.3 Exploring biomechanical strategies through optimal control in trampoline

Charbonneau Eve¹, Bailly F.² & Begon M.¹

¹*Laboratoire de simulation et modélisation du mouvement, Université de Montréal, Canada*

²*Institut national de recherche en informatique et automatique, Université de Montpellier, Montpellier, France*

eve.charbonneau.1@umontreal.ca

The biomechanics of twisting somersaults is not intuitive since it involves high-rate rotations about multiple axes at the same time. Therefore, computer simulation seems appropriate to help coaches innovate as it eliminates injury risks. Our objective is to find innovative twisting somersault techniques through optimal control. We want to extract from series of optimal solutions efficient biomechanical strategies that can be transferred to the field, to help athletes improve their performance. Techniques generated through optimal control produced up to five twists in one backward somersault [1]. By analyzing these optimal techniques, we identified three biomechanical strategies which may help coaches better support their athletes: i) moving segments in the best tilting plane, ii) moving segments in phase with the nutation period and iii) adjusting to converts from twisting mode to somersaulting mode. These are further explained hereafter.

Moving segments in the best tilting plane Twist rotation can be created from strictly somersaulting motions by transferring angular momentum from the somersault axis to the twist axis [2]. In practice, this is accomplished by moving segments (arms and legs) asymmetrically to tilt the body. When the body is already twisting, movements increasing efficiently the twisting rate are three-dimensional as they should happen along the so-called best tilting plane [3] at each instant. This plane is formed by the angular momentum vector and the twist axis. Therefore, coaches should not refrain three-dimensional segment motions.

Moving segments in phase with the nutation period During aerial twisting somersaults, the tilt angle oscillates with a period of half a twist [4]. The amplitude of these oscillations depends on the inertia of the body. This means that it is possible to change the minimum and maximum tilt angle at each oscillation by changing body configuration at each quarter twist. Therefore, coaches should recommend athletes to move segments at each quarter twist position to increase or decrease the twist rate.

Adjusting to convert from twisting mode to somersaulting mode All rotating rigid bodies can only be in two modes of rotation; the twisting or the wobbling mode [5]. In our case, the athlete in twisting mode is simultaneously somersaulting and twisting and the athlete in wobbling mode is somersaulting and has little to large twist and tilt oscillations. Athletes can change their body configuration in the air to switch from one mode to the other. We observed that the inertia changes implied by the transition from a straight position to a pike position are not always sufficient on their own to transfer from twisting to wobbling mode; additional adjustments are needed. Therefore, coaches should encourage their athletes to take time to reposition before piking instead of pushing them to twist and pike as fast as possible.

References

- [1] Bailly, F., Charbonneau, E., Danes, L., & Begon, M. *Multibody System Dynamics*, **52**, 193-209 (2021).
- [2] Yeadon, M. R. *Journal of Sports Sciences*, **11**, 209-218 (1993).
- [3] Charbonneau, E., Bailly, F., Danes, L., & Begon, M. *Applied Sciences* **10**, 8363 (2020).
- [4] Yeadon, M. R. In *Proceedings of the Fourth International Symposium on Computer Simulation in Biomechanics*. (1993).
- [5] Yeadon, M. R. *Journal of Sports Sciences*, **11**, 187-198 (1993).

4.4 Assessment of Different Underwater Undulatory Swimming (UUS) Strategies using a Two-Dimensional CFD Method

Audot Dorian, Thompson I. M., Banks J., Hudson D. & Warner M.

Performance Sports Engineering Laboratory (PSEL), Maritime Engineering group, University of Southampton, University Road, Southampton, Hampshire, SO17 1BJ, United Kingdom

d.a.g.audot@soton.ac.uk

In competitive swimming, after dives and turns, athletes perform underwater undulatory swimming (UUS), copying marine mammals' method of locomotion. The body, performing a wave-like motion, accelerates the fluid downstream in its vicinity, generating propulsion with minimal resistance. Through this technique, swimmers can maintain greater speeds than surface swimming and take advantage of the overspeed granted by the dive (or push-off). Almost all previous research has considered UUS when performed at maximum effort and critical parameters to maximize UUS speed are frequently discussed. However, this does not apply to most races. In only 3 out of the 16 individual competitive swimming events are athletes likely to attempt to perform UUS with the greatest speed, without thinking of the energetic cost of locomotion. In the other cases, athletes will attempt to maximize the speed of their underwater swimming whilst considering an energy expenditure appropriate to the duration of the event. Hence, there is a need to understand how swimmers adapt their underwater strategies to optimize the speed within a limited allocated energetic cost.

This paper develops a consistent methodology that enables different sets of UUS kinematics to be investigated. These may have different power input and force generation mechanisms (e.g. force distribution along the body and force magnitude). The developed methodology therefore needs to: (i) provide understanding of the UUS propulsive mechanisms at different speeds, (ii) investigate the key performance parameters when UUS is not performed solely to maximize speed, (iii) consistently determine the power input of a UUS technique. The methodology developed in order to reach these three objectives is divided into three steps: kinematic data acquisition, processing the kinematic data and Computational Fluid Dynamics (CFD) analysis.

The kinematic acquisition consists of gathering the position of several joints along the body and their sequencing. The data were obtained by video digitization or by underwater motion capture (Qualisys system). During data acquisition, the swimmers were asked to perform UUS at a constant depth in a prone position at different speeds: maximum effort, 100m pace and 200m pace. The kinematic data for every trial are then prepared and each joint's position is fitted with a simple function. Following this, the coefficients of the fitted functions are imported to a fluid mechanics solver (LilyPad) in order to recreate the motion of the swimmers. The solver resolves the flow and the forces resulting from that motion. The CFD solver consists of a two-dimensional Large Eddy Simulation (LES). LilyPad is suitable for swimmers performing UUS as it was written in order to perform quick simulations of moving bodies.

This straightforward approach enables a relatively fast computation and allows simulations to be performed with an inflow velocity that updates regarding the resultant of the longitudinal forces at every time-step. From this methodology, a consequent number of parameters can be computed such as the simulated sustained swimming, the power input by the swimmer's motion, the successive acceleration and deceleration within a kick cycle or the force distribution along the body. Validation of the methodology is achieved by comparing the data obtained from the computations with the original data (e.g.: sustained swimming speed). This method is applied to the different kinematic datasets. Results will include and compare the natural response to pacing instructions of two university level athletes.

4.5 Rowing Race Strategy : find the optimum through hydrodynamics, biomechanics and physiologics constraints.

Cohen Caroline, Boillet A., Dode A., Clanet C., Colard T., Diry A., Maciejewski H. & Messonnier L.

LadHyX, Ecole polytechnique

caroline.cohen@polytechnique.edu

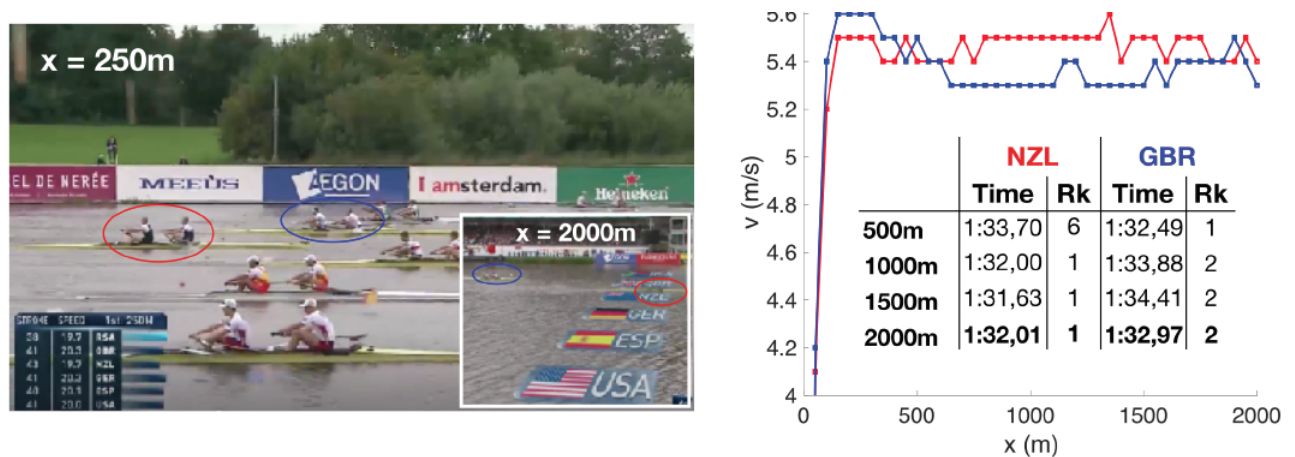


Figure 8: *Illustration of two different strategies during a rowing race (classical GBR vs negative split NZL).*

During a race, rowers have to travel a constant length of 2000 meters. They do it in approximately 240 strokes, oscillating on a thin shaped boat while pulling their oars. During this 6 to 7 minutes effort, they have to choose their energy managing strategy: most of them start very fast but are unable to maintain the high pace until the end of the race; on the contrary, some others accept to start behind in order to have enough energy to finish faster (negative split strategy). Inspired by the seminal work of J.B. Keller on running races [1], the goal of this study is to derive a theoretical model of the rowing race, taking into account hydrodynamic propulsion of the oars [2], hydrodynamics frictions on the rowing boat (added mass, skin friction, wave resistance), and the biomechanics and physiology of the human pforce and velocity generation [3], in order to find the optimal strategy to run the race.

*This work benefits from a State grant managed by the Agence Nationale de la Recherche in the name of Programme d'Investissements d'avenir referenced as ANR-20-STHP-0006 THPCA2024.

References

- [1] Keller J. B. The American Mathematical Monthly, **81(5)**, 474-480 (1974)
- [2] Labbé, R. et al. New Journal of Physics **21.9**, 093050 (2019)
- [3] Kleshnev, V. International research in sports biomechanics. 224-230 (2002)

5 Keynote 2: Running at Altitude: the 100-metre Dash

Monday 6 December - 17h00

di Prampero Pietro Enrico

University of Udine, Italy

pietro.prampero@uniud.it

Theoretical 100 m performance times of a top athlete at Mexico City, Alto Irpavi (Bolivia) (2,250 and 3,340 m a.s.l.) and in a science fiction scenario “in vacuo” are estimated as follows. At the onset of the run: i) the velocity (v) increases exponentially with time; hence ii) the forward acceleration (a_f) decreases linearly with v , iii) its time constant (τ) being the ratio between v_{max} (for $a_f = 0$) and a_{fmax} (for $v = 0$). The overall forward force per unit of mass (F_{tot}), as given by the sum of a_f and of the air resistance ($F_a = kv^2$, where the constant $k \simeq 0.0037 \text{ J}\cdot\text{s}^2\cdot\text{kg}^{-1}\cdot\text{m}^3$) was obtained from the actual relationship between the instantaneous values of a_f and v during Usain Bolt’s extant world record (see figure). Since the decrease of k at altitude (due to the reduced barometric pressure, and hence air density) is known, assuming that F_{tot} is unchanged, the relationships between a_f and v at the altitudes in question were obtained subtracting the appropriate F_a values from F_{tot} . The 100 m performance times, as obtained from the resulting v_{max} and τ values in the three conditions considered amounted to 9.515, 9.474 and 9.114 s, as compared to 9.612 s at sea level. Performance times were also estimated from the relationship between overall mechanical power and speed, assuming that at the end of the run (when $a_f = 0$, and $v = v_{max}$) the mechanical power is unchanged regardless of altitude, thus leading to increased v_{max} values because of the reduced power dissipated against the air resistance. Since a_{fmax} (for $v = 0$), which is obviously independent of altitude, is know (see figure), the so obtained v_{max} values, allowed us to estimate the appropriate time constants (τ) and the corresponding performance times which amounted to 9.474, 9.410 and 8.981 s. In conclusion, the rather small difference ($\simeq 0.3 \%$) between the estimated 100 m time (9.61 s) at sea level and the actual 100 m world record by Usain Bolt (9.58 s) supports the validity of the above approach. Hence, neglecting science fiction scenarios, the 100 m performances times of a top athlete at the two altitudes considered can be reasonably expected to be shorter by 1.0 to 1.4 % at Mexico City and 1.4 to 2.1 % at Alto Irpavi, the slight differences (0.43 to 1.46 %) between the two set data obtained from the two different estimates of τ reported above being likely due to the uncertainties in the underlying estimates of k and/or of the mechanical power.

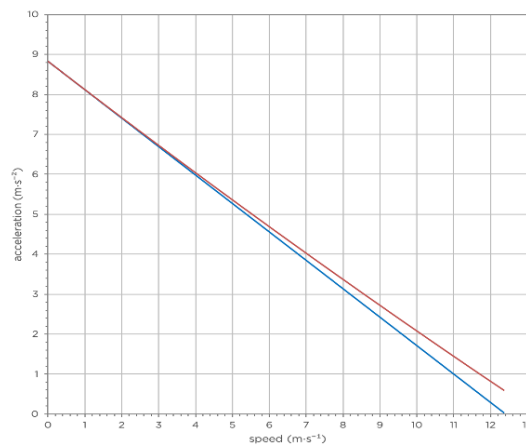


Figure 9: Forward acceleration (a_f , $\text{m}\cdot\text{s}^{-1}$, blue) and overall forward force per unit body mass (F_{tot} , $\text{N}\cdot\text{kg}^{-1}$, red) as a function of the speed ($\text{m}\cdot\text{s}^{-1}$) during Usain Bolt’s world record performance.

6 Keynote 3: Functional Electrical Stimulation Cycling: an Electrifying Sport

Tuesday 7 December - 9h00

Bergeron Vance

Ecole Normale Supérieure de Lyon (Univ Lyon, ENS de Lyon, Univ Claude Bernard, CNRS, Laboratoire de Physique, Lyon, France)

vance.bergeron@ens-lyon.fr

Functional Electrical Stimulation (FES) is a method that uses weak electric fields to trigger action potentials, which provoke nerve impulses leading to muscle contractions. When contractions are properly sequenced, the muscle activity can produce movement which has functional outcomes such as; standing, ambulation, grasp-to-reach and other practical movements. This method is particularly useful to actuate paretic muscles in the physically disabled, allowing them to gain autonomy and improve their health through participation in physical activities.



Figure 10: *Cybathlon 2016 FES Bike Race.* ©NicolaPitaro

7 Session 4: Fluid dynamics 1

Tuesday 7 December - 10h00

7.1 Numerical study of the influence of the spectrum of a turbulent wind on arrow trajectories

Milani Riccardo¹, Cohen C.², Fauchoux A.¹, Ferrand M.^{1,3}, LeFranc Y.^{1,3} & Maddalena T.^{2,3}

¹CEREA, École des Ponts ParisTech, 6-8 av. Blaise Pascal, 77455 Marne-la-vallée

²LadHyX, École polytechnique, Route de Saclay, 91128 Palaiseau

³EDF R&D, 6 Quai Watier, 78400 Chatou

riccardo.milani@enpc.fr

An analytical flight model and the physical characterization of a typical archery arrow is used to simulate the response of the arrow to a real-life-conditions turbulent wind.

The data collected at SIRTA site (*Site Instrumental de Recherche par Télédétection Atmosphérique*, at Palaiseau, France) over several months (January to April 2021) allowed us to recover a detailed characterization of the wind in a complex, real-life site. The findings are in agreement with the classical Kolmogorov theory (see for instance [1]) and they corroborate the results obtained by [2] which investigated the same site.

We then couple this information with the physical characterization of archery derived in [3]. In particular, we retain the equations of motion describing the trajectory of an arrow shot with background wind, and the physical description of an arrow (e.g. aerodynamic coefficients). Choosing a simplified wind form (sinusoidal) modulated by the measured power spectrum data and feeding it to the equations of motion, we are able to numerically quantify the effect of a realistic turbulent wind on the trajectory of an arrow shot in a typical outdoor-competition situation.

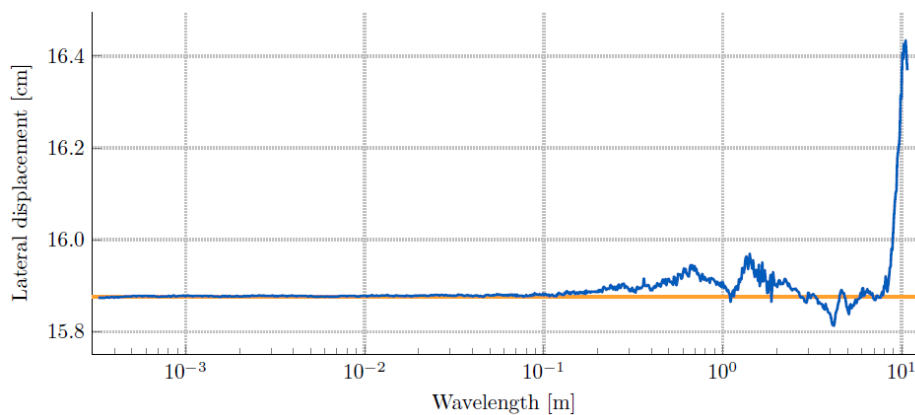


Figure 11: *Lateral displacement at 70m of an arrow submitted to a wind with sinusoidal noise for the wavelengths experimentally measured at SIRTA. The reference displacement computed for a constant wind (no sinusoidal noise) is given in orange*

This project has been supported by EDF Foundation.

References

- [1] Pope S. B., *Turbulent flows*, Cambridge University Press (2001)
- [2] Wei X., *Experimental and numerical study of atmospheric turbulence and dispersion in stable conditions and in near field at a complex site*, PhD thesis, Université Paris-Est (2016)
- [3] Maddalena T., *La physique des sports de tir*, PhD thesis, École polytechnique (2020)

7.2 Wave drag in unsteady motion

Dode Antoine, Carmigniani R., Cohen C., Clanet C. & Bocquet L..

Laboratoire de physique de l'ENS, 24 rue Lhomond, 75005 Paris

antoine.dode@ens.fr

Objects moving at the water surface with a cyclic propulsion move with an unsteady velocity. We report here the experimental and theoretical study of such unsteadiness on the wave resistance. Towing hulls of size L with a sinusoidal speed, the mean drag is measured for different amplitudes, frequencies of the fluctuating velocity, as well as different Froude numbers \mathcal{F}_0 associated with the mean velocity V_0 ($\mathcal{F}_0 = V_0/\sqrt{gL}$). Depending on the Froude number \mathcal{F}_0 , the wave drag is either increased or decreased by velocity fluctuations and depends linearly on the square of their amplitude. The effect is maximum for a resonance frequency identified as the Wehausen frequency $\tilde{\Omega}_r$, scaling like the inverse of the Froude number $\tilde{\Omega}_r \propto 1/\mathcal{F}_0$. All these results are rationalized on the basis of a theoretical framework for the unsteady wave drag which extends Havelock's theory.

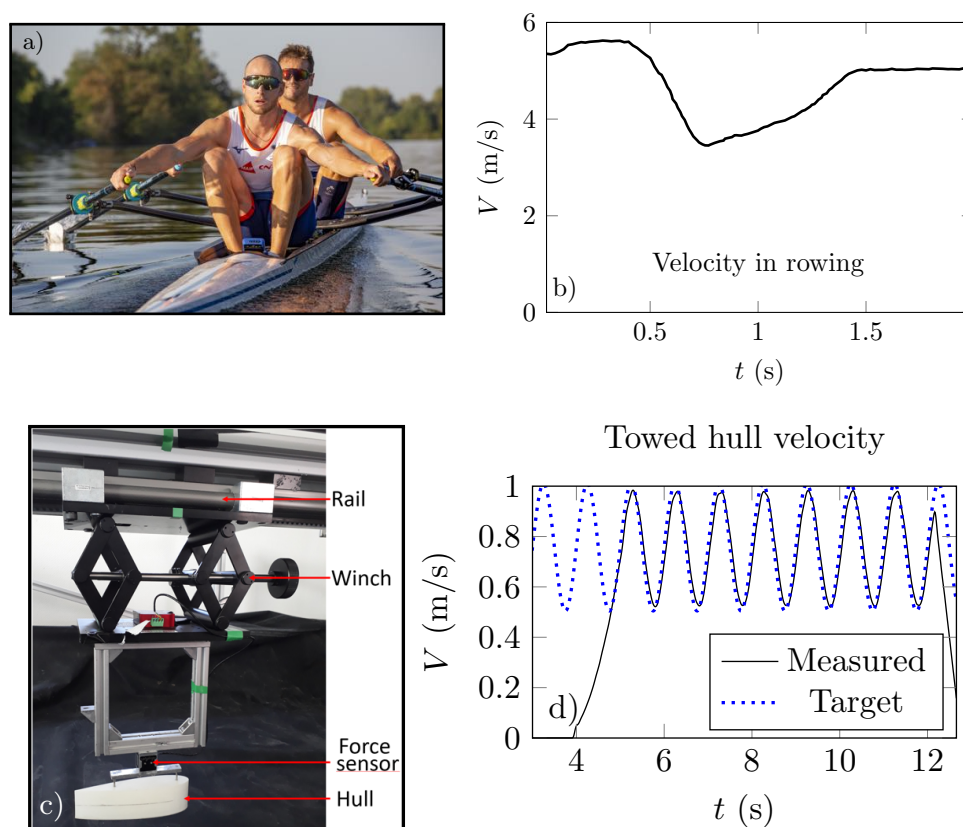


Figure 12: **a)** Example of unsteady regime associated to oar propulsion. Men double sculls (Hugo Boucheron & Matthieu Androdias, FRA, photo: D. Blin, FFA). The wake, visible on the sides of the hull, is related to the velocity of the boat. **b)** Evolution of the speed of a single scull during one propulsion cycle, taken from [1]. **c)** Setup presentation: side view of the system. **d)** Payload velocity during an unsteady measurement.

References

- [1] Kleshnev V., The physics of rowing (2016)

7.3 Cycling aerodynamics

Abel Hector¹, Cohen C.¹, Brunet E.², Robert C.³, Grasso F.³ & C. Clanet¹

¹Ecole Polytechnique, ²Fédération Française de Cyclisme, ³IAT Saint Cyr

Hector.ABEL@segula.fr

Using a wind tunnel equipped with a six components aerodynamic balance mounted on a rotating turntable, we first study the aerodynamic force exerted on a real cyclist in time trial position from head to tail wind limits. The polar curve is deduced and a theoretical model for the aerodynamic force is proposed and compared to other existing data [1]. A CFD model is also developed and compared to both the experiments and the theory in order to explore more delicate configurations such as turns.

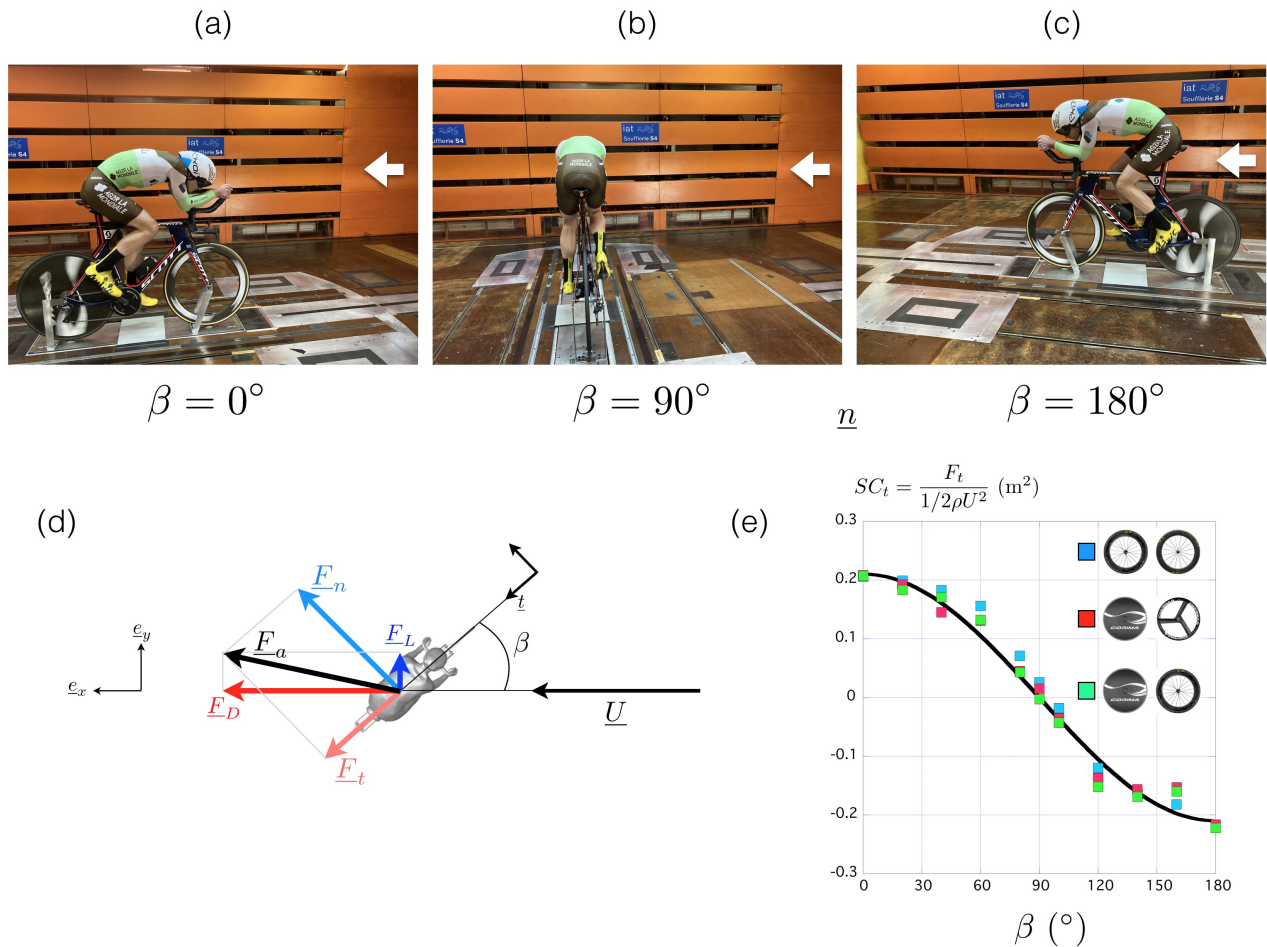


Figure 13: *Experimental set-up used to measure the wind force \underline{F}_a on a cyclist: (a) pure head wind position ($\beta = 0^\circ$), (b) perpendicular wind ($\beta = 90^\circ$), (c) pure back wind position ($\beta = 180^\circ$) (d) conventions used to describe the forces acting on the cyclist. In figures a,b,c, the white arrow indicates the direction of the flow (e) variation of the tangent drag area SC_t as a function of the direction of the apparent wind β for three different wheel sets.*

References

[1] Fintelman D.M., Sterling M., Hemida H. & Li F.-X., *Procedia Engineering*, **72**, 720-725 (2014)

7.4 Cycling in the wind

Clanet Christophe¹, Brunet E.², Roy J.², Plougonven R.¹ & Cohen C.¹

¹*Ecole Polytechnique.* ²Fédération Française de Cyclisme

clanet@ladhyx.polytechnique.fr

The impact of wind on road cycling races has never been studied quantitatively [1]. One possible reason is that the classical expression for the aerodynamic power dissipation is incomplete and only holds for the head and back wind limits [2].

Here we study the Dutch Headwind Cycling Championships and show how the wind speed and direction affect cycling performances. Using \underline{U}_c for the cyclist velocity and \underline{U}_w for the wind speed, we show that the aerodynamic power that cyclists must overcome writes:

$$P_a = -\frac{1}{2}\rho SC_{t0} \sqrt{U_c^2 + U_w^2 + 2U_c U_w \cos \alpha} (U_c + U_w \cos \alpha) U_c \quad (1)$$

where ρ stands for the density of air and SC_{t0} for the frontal drag area. The angle α which appears in this equation defines the direction of the wind with respect to the cyclist: $\underline{U}_c \cdot \underline{U}_w = -U_c U_w \cos \alpha$ (headwind corresponds to $\alpha = 0$).

This expression of the aerodynamic power together with precise meteorologic data allow us to develop a theoretical model to understand the best performances observed during these windy races.

The comparison with the actual final results for both men and women records are in fair agreement for all the six editions of the race.



Figure 14: *Cyclist during the 2015 edition of the Dutch Headwind Cycling Championship (NK Tegenwindfietsen).*

References

- [1] Cohen C, Brunet E., Roy J. & Clanet C., J. Fluid Mech. **914**, A38 (2021)
- [2] Malizia F. & Blocken B., J. of Wind Engineering & Industrial Aerodynamics. **200**, 104134 (2020)

7.5 Shaping your hand for more efficient swimming

van de Water Willem¹, van den Berg J.², Bazuin R.¹, Jux C.², Sciacchitano A.², & Westerweel J.¹

¹Department of Mechanical Engineering, Laboratory for Aero and Hydrodynamics, ²Department of Aerospace Engineering, Delft University of Technology

w.vandewater@tudelft.nl

How to hold your hand in front crawl swimming? Should it be flat or curved? By shaping your hand, hydrodynamic drag can be maximized, which increases propulsion efficiency.

It is now accepted the fingers should be slightly spread [1]. From the analogy with the well-known cup anemometer, one might expect that that cupping the hand also helps in increasing drag. What about the thumb; should it be spread (abducted) or not?

We measure drag in a stationary flow. Swimming is in water, but using Reynolds similarity the drag experiments are done in a wind tunnel. We obtain accurate forces on real-life models of a forearm with hands, flexing the thumb and fingers in various positions. The effects are expected to be small (a few percent), but in professional swimming they can make the difference between a gold medal and no medal at all. Therefore, we need precise and well-controlled experiments.

We study the influence on drag of cupping the hand and flexing the thumb. We find that cupping the hand is detrimental for drag. Swimming is most efficient with a flat hand (and slightly spread fingers). Flexing the thumb has a small effect on the drag, such that the drag is largest for the opened (abducted) thumb. Flow structures around the hand are visualized using robotic volumetric particle image velocimetry. From the time-averaged velocity fields we reconstruct the pressure distribution on the hand. In the figure, these pressures are compared to the result of a direct measurement. The reached accuracy of $\approx 10\%$ does not yet suffice to reproduce the small drag differences between the hand postures.

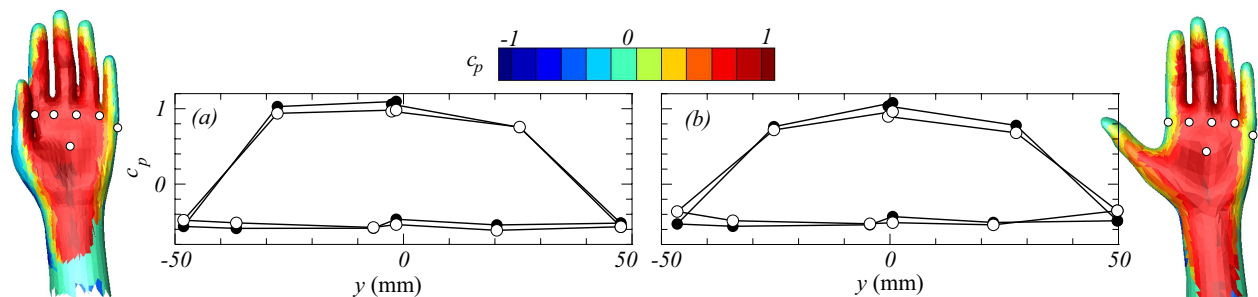


Figure 15: Pressure distribution on the palm side of hands with adducted (left) and abducted (right) thumb. It was computed from the measured 3D flow field and Reynolds stresses. Frames (a,b) are a comparison between the pressures from PIV (open circles) and those measured with a pressure sensor (closed dots). The pressure taps on the palm side of the hand are indicated. Those at the back of the hand are approximately at the same z - (vertical) location.

References

- [1] J. van Houwelingen, D. H. Willemsen, R. P. J. Kunnen, G. F. van Heijst, E. J. Grift, W. P. Breugem, R. Delfos, J. Westerweel, H. J. H. Clercx, W. van de Water, *J. Biomechanics*, **63**, 67 (2017).

8 Session 5: Energy

Tuesday 7 December - 11h50

8.1 Optimal Individual Pushing Position in Rugby Scrum

Lallemand Benjamin^{1,2}, Cohen C.¹, Vincent Q.², Blanchard S.², Rouillon S.² & Clanet C.¹

¹ *LadHyX, École polytechnique, Palaiseau, France*

² *Racing 92, Le Plessis-Robinson, France*

benjamin.lallemand@racing92.fr

In rugby games, after a minor infringement or stoppage, scrums are contests of eight players of each team that are pushing collectively to win the ball possession. In order to maximise the sustained force produced by a pack after the phase impact, it is interesting to work and optimize the individual force production of forward players [1,3].

So, we build an instrumented individual scrum machine in order to study optimal position by measuring pushing forces and by video recording players with top and side views. We develop a protocol to conduct the optimal position study, but rather than studying force production by varying the pushing height h , we study it with respect to the length l represented on figure 16.a.

For each length l , the player modifies his joint angles. When we compute mean sustained active forces F_x for each l for two different professional players, we obtain the graph shown on figure 16.b.

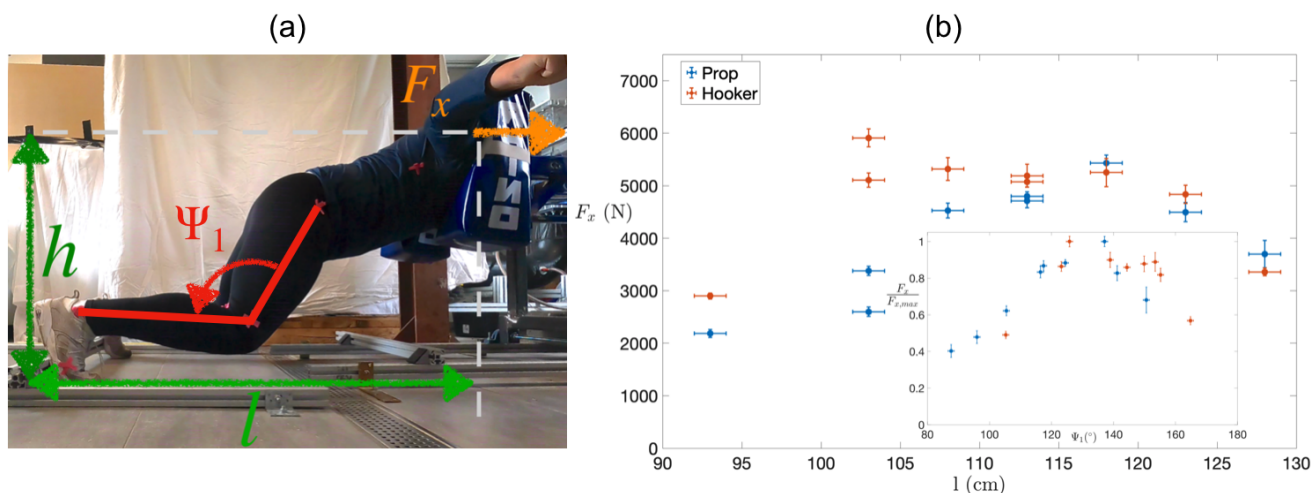


Figure 16: (a) *Professionnal player pushing on the instrumented scrum machine.* (b) *Experimental sustained force F_x according to l .*

A different optimal l is identified for the two players. Furthermore the curve's shape of the hooker is flatter than the prop one. By plotting these F_x forces with respect to the knee angle Ψ_1 (cf figure 16.b), the two experimental curves are collapsing and they define what seems to be an optimal angle that maximize the force production. Finally, we develop a biomechanical model in to account for these experimental observations.

References

- [1] Martin E.& Beckham G., BMC Sports Science, Medicine and Rehabilitation, **12**, 33 (2020)
- [2] Wen-Lan W., Jyh-Jong C., Jia-Hroung W. & Lan-Yuen G., Journal of Strength and Conditioning Research, **21**(1), 251–258 (2007)

8.2 Energies and forces during pole vault flight

Lustig Quentin¹, Homo S.², Brisard S.³, Clanet C.⁴, & Carmigniani R.¹

¹Ecole des Ponts, EDF R&D,² French Athletics Federation,

⁴Université Gustave Eiffel, ⁴Ecole Polytechnique

quentin.lustig@student-cs.fr

When looking at the evolution of the world records and yearly best performances of world class pole vault jumpers, we observe a stagnation of the best performance below the 6.20 m mark, with a current world record held by Armand Duplantis at 6.18 m. Yet, on closer inspection, the number of athletes able to pass the 6.10m mark is small (only 3 in the world, fig.17-a). How to explain such a difference in level ? In the present study, we aim to quantify the energy transfers (fig.17-b) and the interaction forces between the athlete and the pole during an international competition.

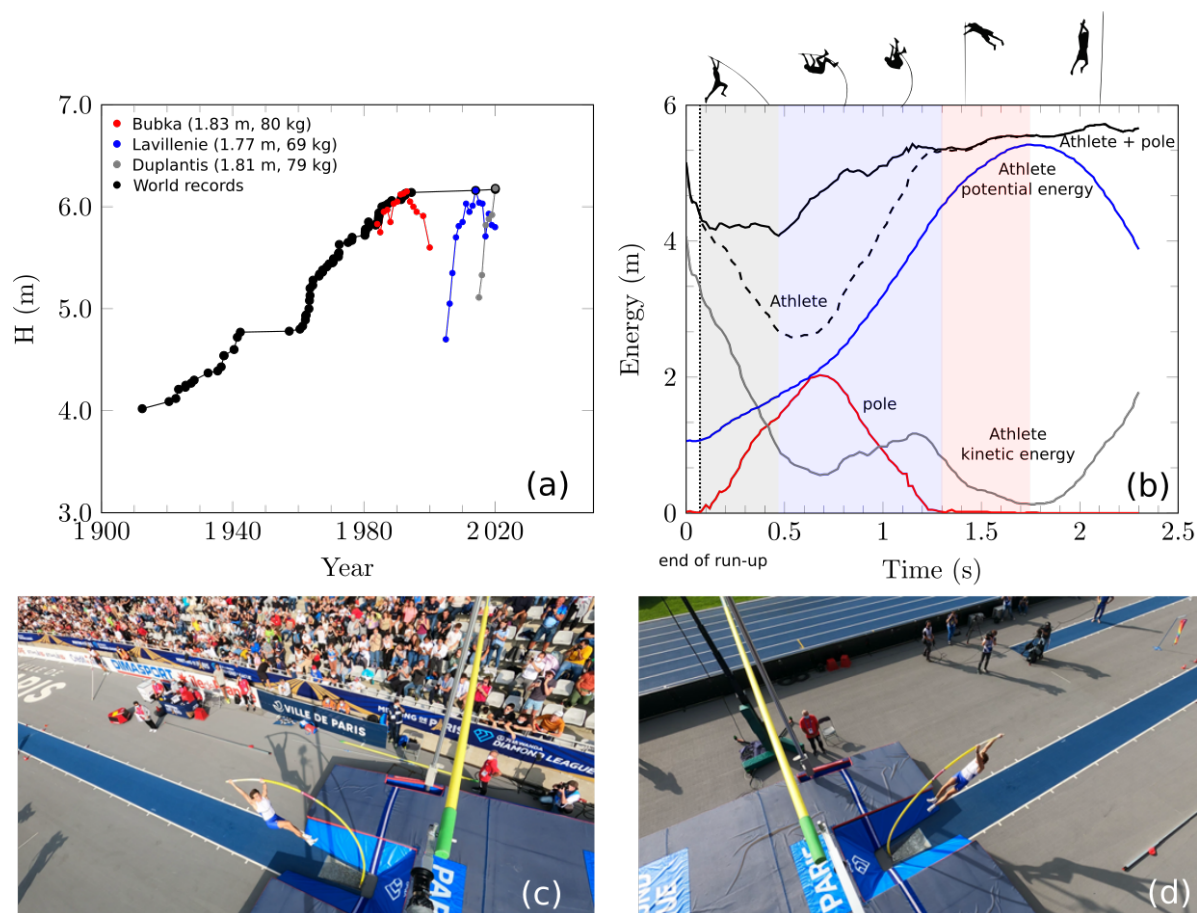


Figure 17: (a) Evolution of the world record in pole vault and yearly best performances of three jumpers. (b) Evolution of the energies measured during vaulting. (c)-(d) Two views of a pole vault from the standards.

To this end, during the Paris Diamond League in August 2021, we used two cameras attached on top of the pole vault standards (fig. 17-c&d). Over 80 jumps were recorded and one jump exceeded the 6m mark. The scene is calibrated and triangulation makes it possible to deduce the 3D deformation of the pole and trajectory of the athletes. A quasi-static approach is used to evaluate the energy stored in the pole and the forces between the pole and the jumper during the jump. Figure 17-(b) shows the evolution of the measured energies during one practice jump of a French pole vault athlete. Our findings confirm that a significant part of the potential energy at release is due to the jumper activity after take-off (in the present case about 20%). This analysis also makes it possible to identify different important phases of the vault for which the athlete inputs or loses energy. These successive phases can be qualitatively observed by the coach. We now provide a methodology to *quantify* these phases. A similar analysis of the dynamics of vaulting will also be discussed.

8.3 Looking for optimal biomechanical configurations in weightlifting and powerlifting

Vedel Charlotte, Bou-Saïd B. & Dureisseix D.

Université de Lyon, CNRS INSA-Lyon, LaMCoS, UMR5259, F-69621 Villeurbanne, France

charlotte.vedel@insa-lyon.fr

More than sports, weightlifting and powerlifting are widely used in fitness/resistance training for sport performance. As they both consist of lifting additional weights they must be well executed to avoid injuries and enhance fitness and performance. To date, pieces of advice from experienced or graduated or self - proclaimed coaches, swarm in gyms and on the web, but very little are based on scientific knowledge [1]. The same technical instructions are often given to men and women with different anthropometry and training history. As they are not individualized, these instructions could be at best suboptimal for most athletes, not enabling them to express their full potential and, at worst, dangerous and causing injuries. The central objective of our project is the development of an optimised personalized virtual human model. The goal is the optimization of performance with an assessment of injury risks at the limits of performance.

On the one hand, a virtual mechanical/skeleton model of an athlete squatting was numerically designed and set in motion according to the International Powerlifting Federation rules [2]. Anthropomorphical determinants measured by bi-planar radio (EOS) of one of the top French elite lifters were used in the model to make it as realistic as possible. The efficiency of the movement was then evaluated through a fitness function found in the literature [3] and a genetic algorithm was finally designed to find a pattern maximizing this function . On the other hand, an analysis of the existing tools to capture movement in training was made and an experiment was designed to assess with a force plate the motion of the center of pressure through the squat movement. The results of the modelization and experimentation were then compared.

Currently, it seems that the centre of gravity displacement along the lift of all the subjects is the opposite of the mechanical optimum found with the genetic algorithm. In fact, elite athletes tend to have their center of pressure move forward during the eccentric part of the lift and backward during the concentric one while the mechanical model tends to have the opposite pattern. This difference could be explained either by the muscular strategy used by athletes -forward center of pressure means greater knee extensors recruitment during the concentric phase- or by the central nervous system preventing the muscles from contracting when the equilibrium is unstable. Even if elite athletes may not have optimal movement, the fact that the centre of gravity moved according to the same pattern for all of them suggests that the model must be completed. To do so, a better understanding of the mechanisms involved in the squat lift is necessary.

References

- [1] International powerlifting federation, Technical Rules Book, **17** (2021)
- [2] Leboeuf Fabien, Patrick Lacouture, Construction et illustration des différentes formulations biomécaniques du coût énergétique d'un geste sportif, 37-52 (2008)
- [3] Ho, Lester K.W., Lorenzen & al., Journal of Strength and Conditioning Research Reviewing current knowledge in snatch performance and technique: the need for future directions in applied research, **574** (2014)

8.4 Bike tire rolling resistance

Clanet Christophe¹, Labbé R.², Boucher J.P.², Péraud J.C.³, Brunet E.³, Comtet J.⁴

¹Ecole Polytechnique ²Phyling ³Fédération Française de Cyclisme ⁴ESPCI

clanet@ladhyx.polytechnique.fr

Due to its transport applications, the special case of pneumatic tire rolling friction has been the subject of many engineering studies all underlying the difficulty of the measurement and the lack of general theory [1]. Looking for an heuristic formula for the rolling resistance force, F_{RR} , the Michelin engineer P.S.Grover proposed in 1998 the following expression [2]:

$$F_{RR} = K_F p^{\alpha_p} (Mg)^{\alpha_M} V^{\alpha_V}, \quad (1)$$

where K_F is a constant which depends on the tire type, p the inflation pressure, Mg the load, V the velocity and α_p , α_M , α_V the associated exponents. For a given tire, the following values are obtained: $\alpha_p = -0.345$, $\alpha_M = 0.929$, $\alpha_V = 0.307$. These values underline the decrease of the rolling resistance with an increasing inflating pressure, and a decreasing velocity. It is interesting to notice that with $\alpha_V = 0.307$, equation (1) predicts that the rolling resistance force vanishes at $V = 0$ when there is no rolling, which is what we expect physically. These values of the exponents also point out an almost proportionality of the rolling resistance with the load ($\alpha_M \approx 1$). This observation induced the introduction of the coefficient of rolling resistance $C_{RR} = F_{RR}/Mg$.

We develop a pendulum tribometer which allows to measure the rolling resistance of bike tires (figure 18). This tribometer is used to determine the influence of the nature of the tire, of the inflating pressure, of the velocity, of the load and of the camber of the tire with respect to the road. This experimental study is completed by a theoretical analysis which provides a theoretical expression for the coefficient of rolling resistance.

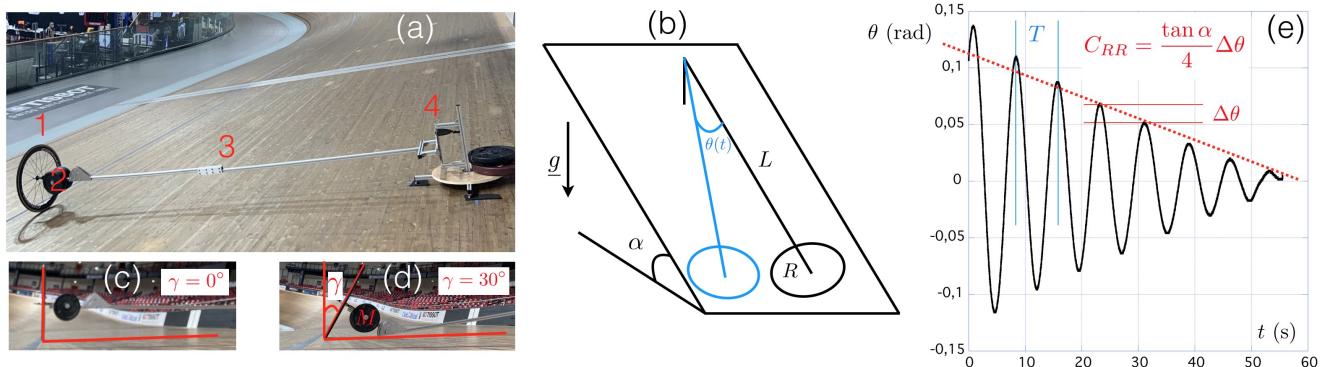


Figure 18: *Pendulum tribometer: (a) picture of the set-up with key parts: 1 is the wheel equipped with the tested tire, 2 is the loading mass, 3 is the rigid shaft and 4 is the axis of rotation (b) operating principle and nomenclature (c) side view with a zero camber angle $\gamma = 0^\circ$ (d) side view with a camber angle $\gamma = 30^\circ$ (e) experimental evolution of the oscillating angle θ obtained with a Vittoria tire inflated at 14 bars and loaded with 30 kg without camber $\gamma = 0^\circ$.*

References

- [1] D. Schuring, Rubber Chemistry and Technology **153**, 600-727 (1980)
- [2] P.S. Grover, International Congress & Exposition. SAE International, 400 Commonwealth Drive, Warrendale, PA, United States (1998)

9 Session 6: Fluid dynamics 2

Tuesday 7 December - 14h00

9.1 Velocity–Stroke rate in paddle sports

Carmigniani Rémi¹, Prétot C.¹, Violeau D.¹, Cohen C.², Clanet C.²

¹LHSV, ENPC, EDF R&D,²LadHyX, Ecole Polytechnique

remi.carmigniani@enpc.fr

In swimming and kayaking (figure 19.a), athletes use paddles to propel themselves near an air-water interface. In the case of swimming, the paddles correspond to the swimmer's hands. To vary their mean velocity (V), they mainly change the rate of execution of a propelling movement with their paddles, call stroke rate (SR). To study this velocity–stroke rate relationship, athletes in different *paddle sports* were asked to maintain a constant speed for about 5 seconds on 10 consecutive trials with sufficient rest to neglect effect of fatigue. The only constraint was to increase the velocity at each trial from the lower at trial number 1 to the fastest velocity they could achieve in trial number 10. We measured the mean velocity and the stroke rate as shown in figure 19.b).

An increase of the stroke rate leads to an increase of velocity. In swimming, this relationship is close to $V \propto SR^{1/2}$ [1], while in kayaking we observe a relationship as $V \propto SR^{1/3}$ [2]. In the present work, we propose a general model to explain the evolution of the velocity with stroke rate in *paddle sports*.

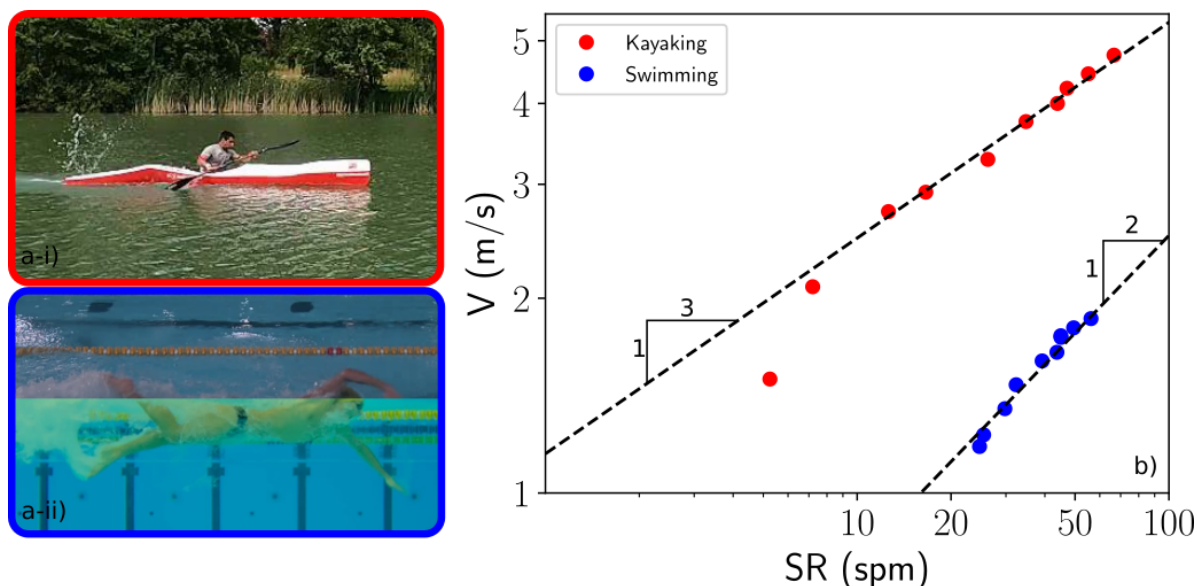


Figure 19: (a) Examples of paddle sports : i) kayaking and ii) swimming. (b) Evolution of the velocity as a function of the stroke rate in swimming (blue) and kayaking (red).

This work was supported by the ANR NePTUNE (ANR-19-STHP-0004), the ANR THPCA2024 (ANR-19-STHP-0006) and the EDF Foundation.

References

- [1] R. Carmigniani, L. Seifert, D. Chollet and C. Clanet, *Coordination changes in front-crawl swimming*, RSPA, 2020
- [2] C. Prétot, L. Hasbroucq, R. Carmigniani, R. Labbé, J.P. Boucher, C. Clanet, *Physics of kayak races*, RSPA, 2022 (submitted)

9.2 Getting a boost from shallow water

Benham Graham P.¹, Bendimerad R.², Benzaquen M.³ & Clanet C.³

¹*University of Cambridge*, ²*Cornell University*, ³*Ecole Polytechnique*.

gpb35@cam.ac.uk

Rowing race courses usually have a minimum depth requirement of 3m, but with boats as long as 18m, rowers are likely to generate waves in both the deep (dispersive) and shallow (non-dispersive) regimes during a race. In fact, regions of shallow water may either *reduce* or *enhance* the wave drag of the boat, depending on the specific parameter values (e.g. the length and speed of the boat) [1].

In this talk, I will demonstrate both experimentally (using measurements from a tow-tank) and theoretically (using linear wave theory [2]), that as the rowing boat moves into a region of shallow water, two possible cruising speeds emerge - one faster (supercritical) and one slower (subcritical). Hence, in a race with variable water depth there are certain moments where rowers can alter their strategy to gain competitive advantage over their opponents.

Perspectives from this work include optimising rowing power over the course of a race with varying bathymetry, taking into account the fixed energy budget of the athletes. Comparisons are made with racing data, and we discuss whether such effects may have played a role in past Olympic Games.



Figure 20: *Rowing race at Lake Bled, Slovenia (Image from redbull.com)*

References

- [1] G.P. Benham, R. Bendimerad, M. Benzaquen & C. Clanet, *Phys. Rev. Fluids*, **5**, 064803 (2020)
- [2] T. Havelock, *Proc. R. Soc. Lond. A*, **95**, 354 (1919)

9.3 Optimal swimming start

Prétot Charlie¹, Belhadji K.², Clanet C.² & Carmigniani R.¹

¹ LHSV, Ecole des Ponts, EDF R et D

² LadHyX, Ecole polytechnique

charlie.pretot@polytechnique.edu

In competitive crawl and butterfly, swimmers start on blocks outside the pool, dive and are allowed to swim underwater up the 15 meters marks. This initial phase is crucial for short races (50 m, 100 m) as it can represent up to 30% of the total race distance. We analyse the start of 7 french top-level swimmers. Among them, 4 went to Tokyo's Olympics in 2021 and the 3 others are national level.

In this work, we study the trajectory of the swimmers' center of mass. These trajectories are obtained using 6 aerial and submarines views, synchronised and calibrated to reconstruct the center line of the swimming lane. Fourteen characteristic points are tracked on the swimmer to compute the center of mass position [1].

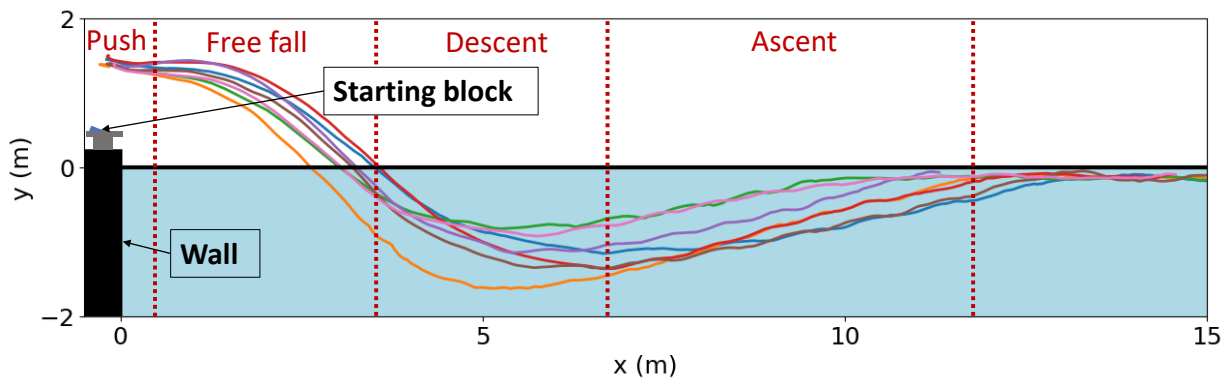


Figure 21: Start's trajectory of the center of mass for 7 different swimmers .

Swimmers can exhibit different trajectories as shown in figure 21. We define four different phases of the start: push, free fall, descent, and ascent. During the free fall, the center of mass follows the well-known ballistic trajectory. The angle of entry in the water is directly related to the push angle and the magnitude of the pushing force on the block. Once the swimmer enters the water, his objective is twofold : being far away from the surface to minimize wave drag and not too far in order to reach the surface quickly at 15 meters. Finally, the slope of the ascent phase depends on the ability of the swimmer to do a dolphin kick.

We first study each phase and then conduct a global optimization of the time needed to reach 15 meters.

This work was supported by the ANR Neptune (ANR-19-STHP-0004).

References

- [1] De Leva Paolo, Journal of Biomechanics **volume 29**, issue **9**, pages 1222-1230 (1996)

9.4 Drafting effect in cycling, a field study

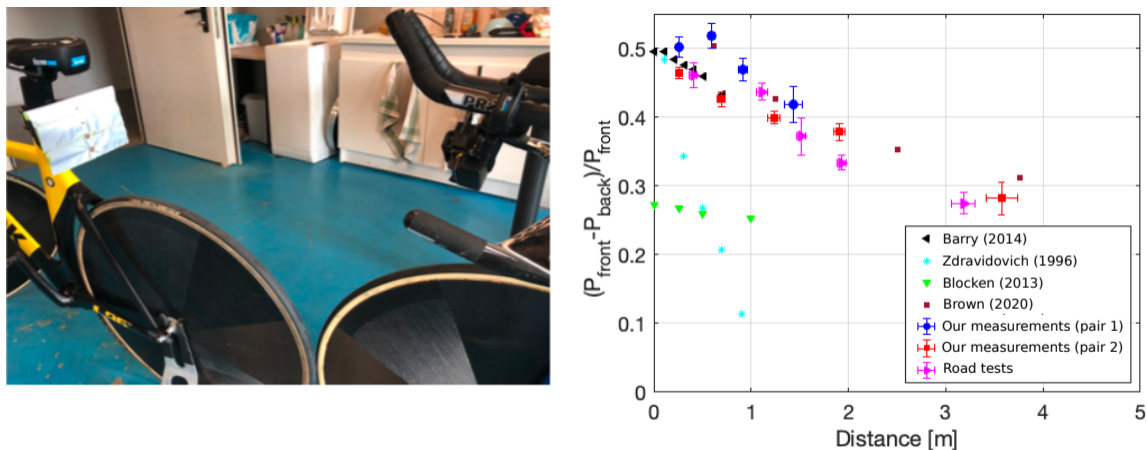
Le Cunuder Anne, Mille A. & Odier P.

Univ Lyon, ENS de Lyon, Univ Claude Bernard, CNRS, Laboratoire de Physique, 69342 Lyon, France

anne.lecunuder@unil.ch

Cyclists riding behind another cyclist have all experienced the well-known “drafting effect” consisting in a significative reduction of the drag force applied by the wind. This effect is used in various team cycling competitions, such as road races or track team pursuit. However, the amount of drag reduction as a function of the distance between cyclists remains an open question. Several studies have tackled this issue either in numerical simulations or in wind tunnels. A number of these results are summarised in the review article by Crouch et al [1]. As can be seen in their figure 14a, these results display a broad variation of the drafting effect with the distance.

In this work, we perform a field study with female junior elite athletes in a velodrome. The athlete riding at the back is equipped with an infrared-distance measuring-device attached to her handlebar, directed towards a target fixed on the seat post of the front athlete (see photo in the figure). At the same time, both athletes are equipped with power meters (*Exakt* pedals from *Look Cycle/SRM*). They are requested to ride at constant speed (between 40 and 50 km/h), while maintaining a given distance between them, varying by increments of distance.



9.5 Drafting of two swimmers

Bolon Baptiste¹, Prétot C.¹, Clanet C.², Larrarte F.³ & Carmigniani R.¹

¹LHSV, ENPC, EDF R&D, ²LadHyX, Ecole Polytechnique, ³Université Gustave Eiffel

baptiste.bolon@enpc.fr

Open water swimming is a tactical sport. As in cycling, competitors often swim in peloton formations. Therefore, their position in the group is crucial to optimize drafting, either to preserve their physical strength, to quickly pass a lead swimmer or to impede the passing of an opponent. Our work is an experimental study of the drag on 2 swimmers scaled models ($L = 40\text{cm}$). It carries on the work of J. Westerweel [1]. The measurements take place in a current flume at EDF Lab and forces are measured using 1D-shear force sensors designed by *Phyling* [2].

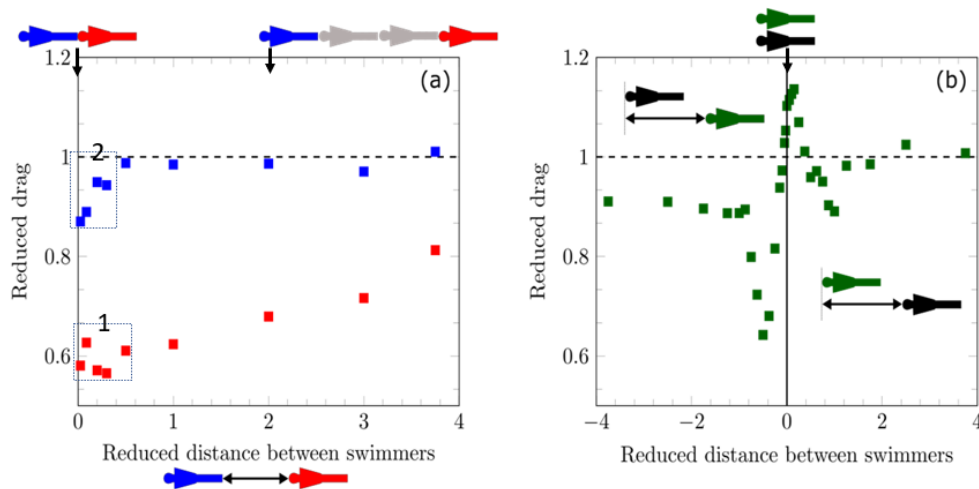


Figure 23: (a) Reduced drag at one given speed in line. (b) Reduced drag at one given speed in alongside swimming. The reduced drag is defined by $(\text{Drag})/(\text{Alone swimmer's drag})$ and reduced distance by $(\text{Distance between swimmers})/(\text{Swimmer's length})$ as shown in the sketches.

First consider two swimmers in line (fig.1-a) and measure the passive drag for different swimming speeds through a Froude similitude to represent both usual speeds during the 10 km race and sprint speed at the end of the race. Froude is defined by $Fr = \frac{V}{\sqrt{gL}}$ and its values are 0.28, 0.34 and 0.38. Concerning the drafted swimmer, his drag force is reduced up to about 40% when just behind the leader (zone 1 in figure 23.a). The further from the leader, the bigger the drag. The leader also experienced a drag reduction when the drafted is directly behind (zone 2 in figure 23.a), but only by about 10% and this effect disappears quickly as the drafted is further away.

Secondly, we study multiple configurations of 2 swimmers being alongside (23.b). Here, we measure both drag and transverse forces, at the same Froude numbers as described above. In terms of drag, it is maximum when swimmers are perfectly side by side. It is minimum when the head of one is 0.5 body length behind the head of the other one (around the hip). That means swimmers should avoid the first position and favor the second one when forced to swim alongside.

This work was funded by the ANR NePTUNE (ANR-19-STHP-0004). We are thankful to EDF Lab for their technical help with the flume.

References

- [1] J.Westerweel, K.Aslan, P.Pennings, B.Yilmaz, *Advantage of a lead swimmer in drafting*, 2016
- [2] Phyling, Drahi-X-Novation Center, <https://www.phyling.fr/>

10 Session 7: Tracking/data analysis

Tuesday 7 December - 15h50

10.1 Automatic detection of stroke phases in front crawl with the use of Dynamic Time Warping (DTW)

Guignard B.¹, Boulanger Jérémie², Seifert L.¹, Letocart A.¹ & Simbaña-Escobar D.³

¹*CETAPS EA3832, Faculty of Sport Sciences, University of Rouen Normandy, France* ; ²*Faculty of Sciences and Technologies, University of Lille, Lille, France* ; ³*Performance Optimisation Department, French Swimming Federation, Clichy, France*

brice.guignard@univ-rouen.fr

In the front crawl, it is possible to calculate a simple temporal index that allows to understand the level of coordination of a swimmer: the index of coordination or IdC [Chollet et al., 2000]. This index measures the time difference between the end of the propulsive action of one of the two arms (start of recovery), compared to the beginning of the propulsive action of the second arm (start of pull). As previous studies only rely on a few number of cycles (3 to 4 on average), this could be done manually. However, more recent studies have sought to identify this cue based on the use of waterproof inertial sensors positioned on the forearms and sacrum. Dadashi et al. (2013) then proposed automatic detections based mainly on angular velocity, but those detections took place at speeds far from the ones of competitions (between 1.06 and 1.17 m/s). At higher speeds such as 1.8 m/s and above, the identification of the beginning of pull is made much more complex (restricted glide, and hence limited plateau in the signal). Comparing two different strokes cycles can be performed with Dynamic Time Warping (DTW, figure 24), which is a well-known approach for measuring time-series similarity, widely applied in gesture recognition [Jeong and Baek, 2021]. With this technique, an average cycle is built to detect the missing points on each stroke cycle based only on a few detections over the trial. The present study exemplifies the benefits of using such a methodology in front crawl, in comparison to previous classic slope detection change algorithms.

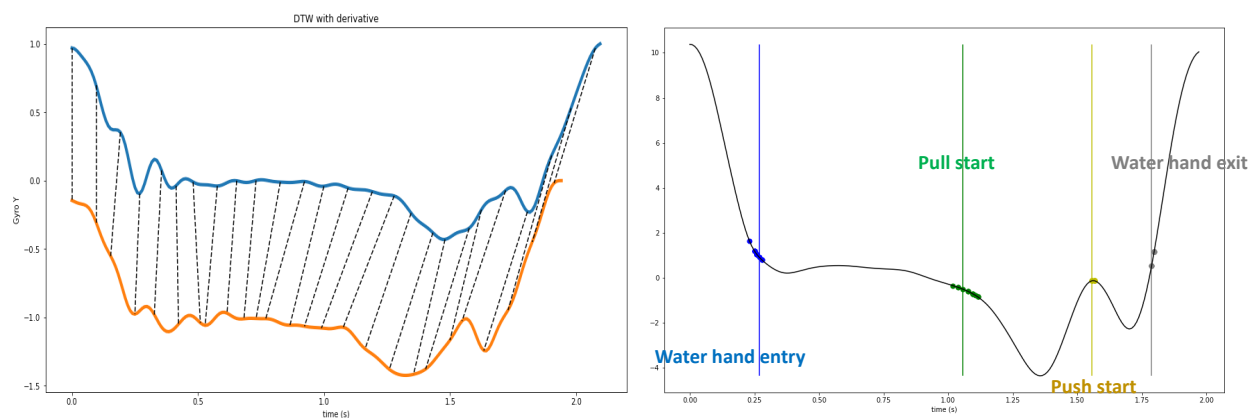


Figure 24: **Left:** two cycles with DTW-based transport between them. **Right:** automatic detections of stroke phases transported onto the average stroke cycle.

This work was funded by the ANR NePTUNE (ANR-19-STHP-0004).

References

- [1] Chollet D. & Chabies S. & Chatard J.C., *Int. J. Sports Med.* **21**(1), 54–59. (2000)
- [2] Dadashi F. & Crettenand F. & Millet G.P. & Seifert L. & Komar J. & Aminian K., *J. Sports Sci.* **31**(11), 1251–1260. (2013)
- [3] Jeong Y-K. & Baek K-R., *Sensors* **21**, 3750 (2021)

10.2 Geometric discrepancies in Olympic windsurf foils: measurements versus athletes' feedback

de La Hougue A.¹, Augier Benoit¹, Iachkine P.², Le Vergos P.¹, Pernod L.³, Sacher M.⁴ & Bot P.³

¹ IFREMER, Marine Structures Laboratory, Plouzané, France

² ENVSN, Quiberon, France

³ IRENav, Naval Academy Research Institute, France

⁴ ENSTA Bretagne, CNRS UMR 6027, IRDL, Brest France

benoit.augier@ifremer.fr

The next 2024 Olympic Games will see a dramatic switch to foiling crafts in the sailing series. IQ foil will then replace the planning RS:X windsurf. Hydrofoils are now widely used to reduce hydrodynamic resistance, leading to increased velocities and sailing crafts performance. However, designing hydrofoils for sailing races remains a complex challenge since the hydrofoil has to achieve flying conditions at the lowest boat speed, while minimizing drag over a large range of boat speeds. Highly-constrained structures, mainly built in carbon fiber composites, represent a good trade-off to address this issue, but lead to an increased sensibility to the mechanical and geometrical parameters of the equipment. These important constraints are due, on the one hand, to the high velocity of the boat for their hydrodynamic component and, on the other hand, to the structural loads. Previous sailing series, as the RS:X, have highlighted the disparities of the fins and the great consequences on their performances, even if all items are supposed identical, because of the limited accuracy of manufacturing. High-level athletes have developed a great ability to feel differences in the behavior of these structures, but it remains a challenge to relate specific characteristics to racing performance. This work is based on an innovative coupled cognitive-physical approach to sport performance and presents an original comparison between Olympic class IQ Foil athletes' feelings relatively to different foils geometries, with numerical simulations. Athletes have assessed three hydrofoils each (six in total) and categorized their feelings in terms of performance (velocity and lift). Simulations are performed on 3D scanned hydrofoil geometries and based on a fast potential approach using an Xfoil-coupled panel method. The comparison of the scanned foils geometries between each other have highlighted some macro differences like wing twist and span length with no clear link with the performance. On the contrary, the simulation results fit perfectly with the athletes feeling, showing the ability of the potential approach to compute some foiling characteristics. Expressed feelings about stability of the system, key to global performance, are however not simulated by this static approach.

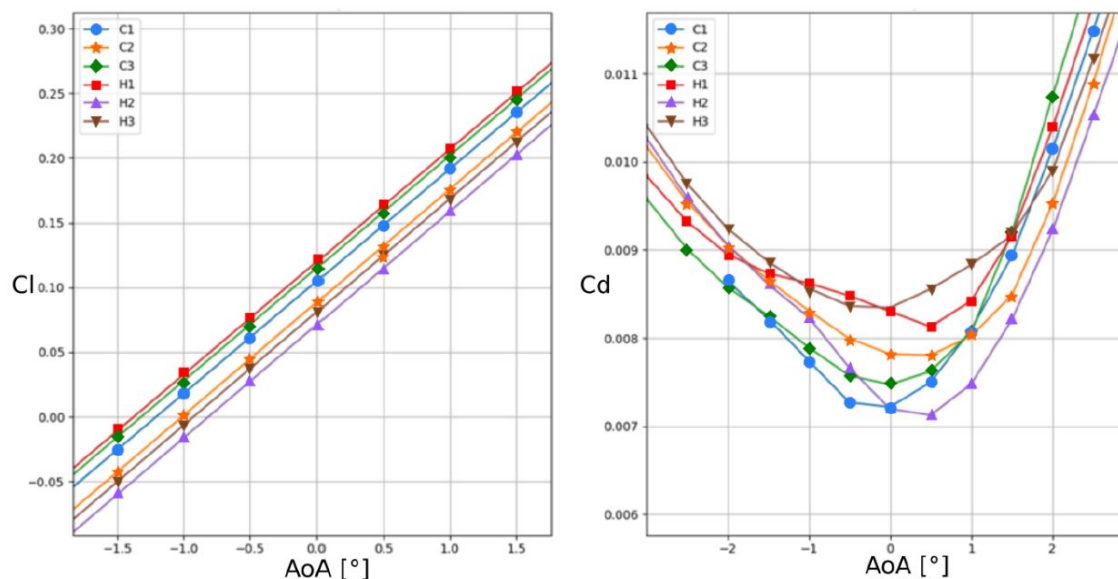


Figure 25: Comparison of simulated lift and drag for the six different hydrofoils considered (Xfoil-coupled Panels method).

10.3 Prediction of wind fields using weather pattern recognition: analysis of sailing strategy and real weather data in Tokyo 2020 Olympics

Banhegyi E.¹, Gorgels S.², Marimon Giovannetti Laura¹ & Pezzoli A.²

¹*SSPA Sweden AB*

²*DIST – Politecnico di Torino and Università di Torino*

Laura.Marimon@sspa.se

The Tokyo 2020 Olympic Sailing Competitions were held in Enoshima bay between the 25th of July and the 4th of August 2021. The climatological and the strategical analysis of the race area for the Swedish Sailing Team was developed in the period included between the three years ahead of the Olympics [1]. The support team was working not only on the forecast but also on the specific analysis of the weather data in the racecourse areas as measured on the water by the Olympics organising authorities and monitored through the SAP Analytics website [2]. Two racecourse areas are herein taken into consideration, namely Enoshima and Zushi, where the Swedish Team athletes sailed most of the races. A statistical metanalysis on the comparison between the forecasted and measured data is carried out, investigating the specific outcome of the strategy of the races with the forecasted metrological data. The Olympic racecourses varied in length and in number of laps, but they all had in common some determined features, such as the start and at least two upwind and two downwind legs for all the ten classes (representing a total of 15 sailor positions/functions). The upwind point of sail is determined as the area close to the wind direction. The closest angle to the wind of each class varies, but all classes feature a series of tacking manoeuvres to reach the first windward mark in a zig-zag-like fashion. The downwind point of sail is situated away from the wind direction, with angles off the wind of approximately 120 to 180 degrees. The strategy of the race can be well set-up during the pre-start time and the first upwind leg, when the top sailors will place themselves ahead of the rest of the fleet. Depending on the class and boats speed and the level of the sailors, some overtakes can happen during the downwind legs and the second upwind. The analysis of the weather data is run along the whole race time, considering all the legs and comparing the results with the forecasted solutions. To have a better strategical analysis, that it is strongly affected by the weather situation, a Decision Support System (DSS), based on the climatic analysis of the racecourses, was developed in the years 2017-2020 [1]. The main component of the DSS is the “call book”, a simple and effective guide designed to help athletes and coaches in the preparation of race strategies. The guide summarizes the meteorological data of the six race fields in tables, plots, and cartographic representations with brief descriptions to be easily understood and quickly consulted both inshore in the months prior to the Olympics and on the venue when training or between races [3]. During the Olympic period, the DSS together with the analysis of the tactics from targeted reference boats allowed to build the confidence on the strategic knowledge, with particular focus on the Medal Race course area. A statistical analysis a-posteriori of the occurrence of the weather patterns for specific race courses also entails the possibility of applying a similar methodology in future Olympic venues.

References

- [1] P. Masino, R. Bellasio, R. Bianconi, A. Besana and A. Pezzoli, “Climatic Analysis of Wind Pattern to Enhance Sailors’ Performance during Races,” *Climate*, pp. 9, 80, 2021.
- [2] SAP Sailing Analytics, “Olympic Summer Games 2020 Tokyo,” 2021. [Online]. Available: <https://tokyo2020.sapsailing.com/>. [Accessed August 2021].
- [3] D. Houghton and F. Campbell, *Wind Strategy*, 3rd edition, London, UK: John Wiley & Sons Inc., 2006.

10.4 An investigation on transfer in motor skill acquisition with machine learning.

Aniszewska-Śtepien Anna, Hérault R., Hacques G., Seifert L. & Gasso G.

LITIS INSA of Rouen and CETAPS Rouen University Normandy Universities

anna.aniszewska@insa-rouen.fr

The evaluation of motor skill learning traditionally relates to compare performances and skills prior and after a period of constant practice. Recent research highlighted the interest of investigating variable practice and of modelling the dynamics of skill learning to better understand individual pathways of learners. Such modelling did not allow any prediction on future performance, both in terms of retention and transfer to new tasks. The present study attempts to quantify, by the means of machine learning algorithm, the prediction of transfer test with two conditions of practice in a climbing task: constant practice (with no changes applied during learning) and variable practice (with graded contextual changes, i.e. the variants of the climbing route). The proposed pipeline allows us to measure adjustment of the test to the dataset, i.e. the ability of the dataset to be *predictive* for the skill transfer test. Despite the difficulty of using the behavioral data in the machine learning framework, we achieved to find a working pipeline.

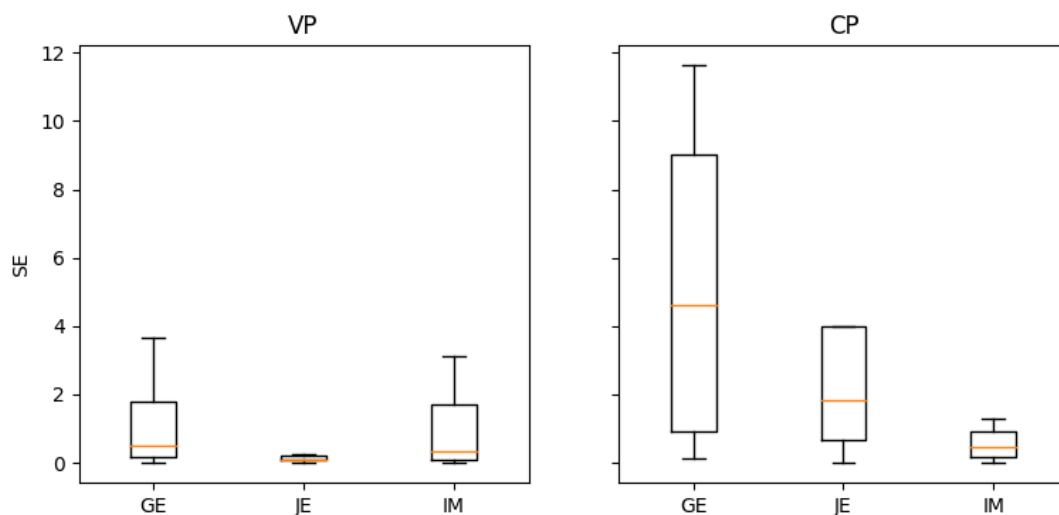


Figure 26: Comparison of the transfer predictivity for variable practice (VP) and constant practice (CP) groups.

In our research, we represented the history of individual performance due to the theoretical findings of the motor learning theory [1] which allows to model the learning progress as the descending exponential. Further, with the parameters of the exponential function fitting, thanks to the usage of the two-stage linear regression model with Lasso selection method [2], we attempted to predict the skill fluency transfer for the two practicing groups separately.

Overall, with our method, we were able to assess the generalisation of learning through the prediction of the outcome on the transfer test. Moreover, we found that the variable practice results in a more stable prediction than the constant one. This supports the importance of variable training for the skill transfer to a new context.

References

- [1] K.M. Newell, G. Mayer-Kress, S. Lee Hong & Y.-T. Liu. Adaptation and learning: Characteristic time scales of performance dynamics. *HumanMovementScience* **28**, 655-687 (2009)
- [2] A. Belloni & V. Chernozhukov. Least squares after model selection in high-dimensional sparse models. *Bernoulli* **19(2)** (2013)

11 Keynote 4: The hydrodynamics of propulsion in rowing

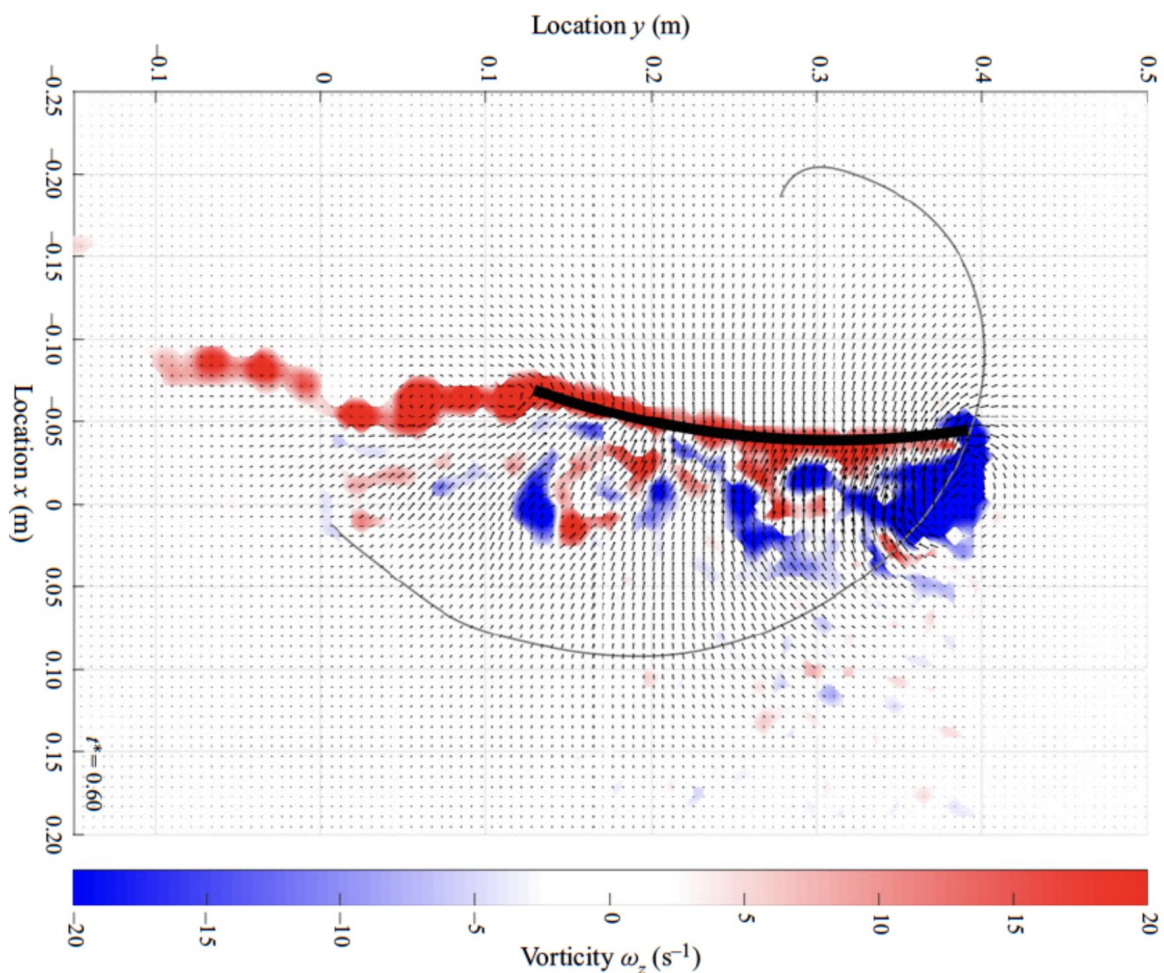
Tuesday 7 December - 17h00

Westerweel Jerry

Delft University of Technology, Laboratory for Aero & Hydrodynamics, The Netherlands

J.Westerweel@tudelft.nl

In order to improve the performance in rowing contests, we built a Ro(w)bot in which we can perform detailed measurements around a 1:2 scale model of an actual rowing blade that moves along a realistic path through water. The set-up allows us to measure both the forces and the impulsive flow by means of time-resolved PIV. We first investigated a more academic case of an accelerating rectangular plate along a straight path, which matches the first stroke at the start of a race. This showed that the forces during the acceleration phase are considerably higher than for steady motion. Also, it demonstrated that there is an optimal depth below the water surface that maximises the drag force. In the second phase of this study we considered the complete motion of an actual rowing blade. This revealed that the generated impulse is not aligned with the propulsive direction, indicating that the propulsion is suboptimal. A simple adjustment is proposed to optimise the alignment of the leading and trailing edge vortices that achieves an improved alignment of the generated impulse with respect to the motion of the boat.



12 **Keynote 5: Understanding the runner-shoe couple mechanics to prevent running-related injuries**

Wednesday 8 December - 9h00

Morio Cédric

Decathlon SportsLab, Lille, France

cedric.morio@decathlon.com

Running is a popular activity which allows anyone to easily achieve its goals, whether wellness, health, or performance. The counterpart to this running craze is the amount of pain and injuries that novice, amateur and professional runners endure each year. A historical point of view to challenge and prevent these injuries was to improve running shoe cushioning [1].

Shoe cushioning has been studied through different aspect: shoe materials properties [2], biomechanical measurements of impact forces [3], physiological assessment like energetic cost of running [4] and even muscle damage estimation [5]. But finally one of the most reliable topics was still the perception of runners [6]. Thus, on these cushioning properties a lot of inferences and speculations have been made and little information are available on the actual influence of shoe cushioning on running related injury [7].

A recent paradigm shift in the footwear research community has been proposed on the individualisation of running shoes recommendations regarding biomechanics and injury prevention [8]. This new paradigm on the individual running biomechanics pattern seems promising. But again it lacks from direct link to running related injuries. In this regards new emerging technologies like inertial motion units [9] and big data computing [10] could help us fill this gap.

References

- [1] Sun X., Lam W.K., Zhang X., Wang J. & Fu W., *Journal of Sports Science and Medicine*. **19(1)**20-37 (2020).
- [2] Lippa N., Hall E., Piland S., Gould T. & Rawlins J., *Procedia Engineering*. **72** 285-291 (2014).
- [3] Potthast W., *Footwear Science*. **3(1)** 1 (2011).
- [4] Shorten M.R., *Journal of Biomechanics*. **26(S1)** 41-51 (1993).
- [5] Hardin E.C. & Hamill J., *Research Quarterly for Exercise and Sport*. **73(2)** 125-133 (2002).
- [6] Delattre N. & Cariou A., *Footwear Science*. **10(1)** 11-19 (2018).
- [7] Malisoux L., Delattre N., Urhausen A. & Theisen D., *The American Journal of Sports Medicine*. **48(2)** 473-480 (2020).
- [8] Nigg, B.M., Mohr M. & Nigg S.R., *Current Issues in Sport Science*. **2** 007 (2017).
- [9] Ruder M., Jamison S. Tenforde A., Mulloy F. & Davis I.S., *Medicine and Science in Sports and Exercise*. **51(10)** 2073-2079 (2019).
- [10] Emig T. & Peltonen J., *Nature Communications*. **11(1)** 1-9 (2020).

13 Session 8: Interaction fluid/surface

Wednesday 8 December - 10h00

13.1 Supercavitating hydrofoil for the World Sailing Speed Record

Ramirez Catherine¹, Papola C.¹, Farnesi M.^{1,2}, Douin X.¹, Cintrat T.^{1,3}, Lanos R.¹ & Bot P.³

¹Syroco, Marseille, France; ²Cubit Innovation Labs, University of Pisa, Italy; ³IRENav, Naval Academy Research Institute, France

catherine.ramirez@syro.co

Syroco is set to tackle the World Sailing Speed Record and aims at reaching a speed of 80 knots with a craft propelled by a wing and anchored in the water by a hydrofoil (see <https://syro.co> and <https://syro.co/en/news/cavitation-test-campaign-irenav-water-tunnel> for the present testing campaign). At such speeds, cavitation (water turning to vapor because of the pressure drop) cannot be avoided on the foil and is often a source of instability, particularly in regimes where cavitation is strongly fluctuating. Then, a strategy is to promote cavitation in order to reach a more stable regime where cavitation is fully developed, and use a foil which is designed to work in this supercavitation regime [1,2]. Typical sections show a sharp leading edge and a blunt trailing edge and supercavitation is achieved when the vapor pocket from the leading edge extends down to the cavity developed at the rear to form a single cavity longer than the section. The CFD simulations needed for the design are challenging and experimental validation is desirable. To this aim, an experimental campaign was performed in the IRENav cavitation tunnel on a typical supercavitating foil section, at Reynolds numbers from 0.8 up to 1.2 million, for cavitation numbers σ ranging from 2 down to 0.24. The flow was visualized with high-speed cameras from the front and from the top. The foil section was fitted with four Fiber-Bragg-Grating sensors on an embedded optic fiber to measure strains, and an FEA analysis was used to infer the corresponding lift force. The different cavitation regimes observed and the corresponding lift coefficients, will be detailed, along with comparison with RANSE simulations.

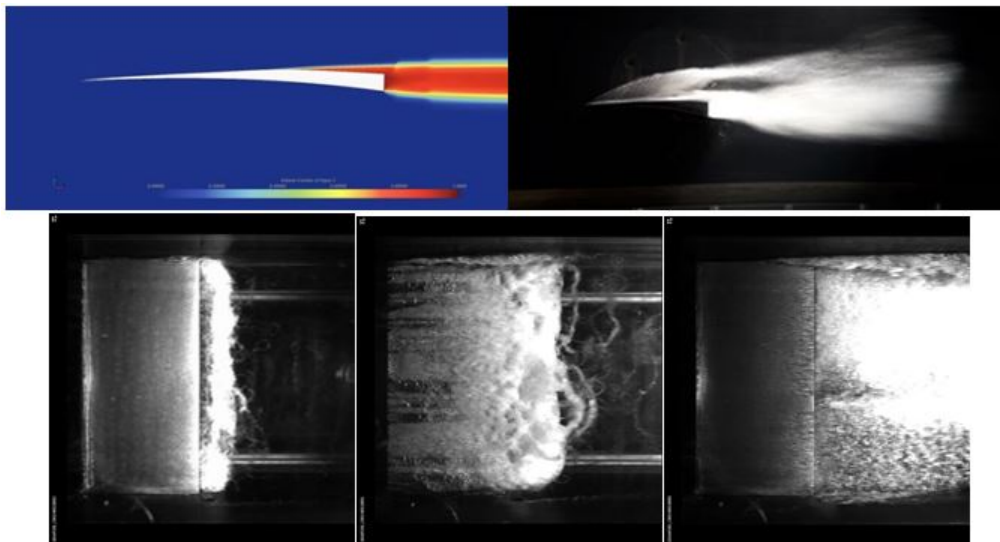


Figure 28: Visualization of a CFD simulation (top left) and experiments in the cavitation tunnel, front view (top right) and top view (bottom), in different cavitation regimes. The flow is from left to right.

References

- [1] Brizzolara S., 4th Int. Symposium on Marine Propulsors SMP'15, Austin, USA (2015)
- [2] Vernengo G., Bonfiglio L., Gaggero S. and Brizzolara S., J. Ship Research **60**, 4, 187-202 (2016)

13.2 The aerodynamic properties of new and worn tennis balls

Choppin Simon, Capel-Davies, J. & Marriott H.

*Sports Engineering Research Group
Sheffield Hallam University
Sheffield, United Kingdom
s.choppin@shu.ac.uk*

This paper follows on initial work presented in 2018 at the International Sports Engineering Conference [1]. The introduction of ball tracking technology in sports such as tennis, baseball and more recently football, has created large sets of trajectory data collected during competition conditions. This data can be used to infer specific behaviour in the sport and represents an alternative approach to traditional scientific investigation [2]. Rather than small, carefully controlled datasets of 100s or even 1000s of trials, modern data sets in sport contain 10s of thousands, 100s of thousands or even millions of trials from which behaviour can be inferred. There may be higher amounts of error within the data and behaviour is unconstrained, but this lack of control can be compensated for by the sheer number of datapoints available. We have access to over 7 years of data from the International Tennis Federation's Davis and Billie Jean King (formerly Fed) Cups. The dataset contains information on ball and player trajectories throughout play. This information was used to investigate whether ball wear significantly affects the aerodynamic properties of the tennis ball.

Early investigations concluded that ball wear *reduces* aerodynamic drag. These investigations have consisted of wind-tunnel tests with new and worn balls. A 'worn' ball has been created by shaving the fluff from its surface [3, 4] but authors have also obtained balls that had been played for 9 games of competitive play [4]. In both cases 'used' tennis balls had a reduced drag coefficient compared to new, and nearly new balls.

Through the use of the Hawk-Eye dataset we have examined drag coefficients measured directly from serve trajectories. by accounting for points in the game when balls were changed, we concluded that used ball have a drag coefficient 4.15% higher than new balls. As this finding was contrary to previous work we have repeated this analysis with a dataset approximately twice the size (due to the increased number of games captured by Hawk-Eye in more recent tournaments). We have also utilised more sophisticated analysis techniques and performed wind-tunnel analysis to confirm our previous findings. Worn balls were taken directly from the Billie Jean King cup and compared to brand new balls using the International Tennis Federation's wind-tunnel. The findings confirm that *newer* balls, not used, have the lowest aerodynamic drag coefficient. While this contradicts previous work in the area, it confirms what players already try to do in competition, where the 'newer' ball is selected prior to the first serve.

We have shown that large data sets in which parameters cannot be tightly controlled can still be used to infer quite subtle behaviour (such as small changes in drag coefficient due to ball wear). Detailed values and approaches will be discussed in the conference presentation.

References

- [1] Choppin, S., Albrecht, S., Spurr, J. & Capel-Davies, J., ISEA 2018 Proceedings **2**, 265-271 (2018)
- [2] Healey, G., Sensors. **21**, (2021)
- [3] Chadwick, S. & Haake, S. Tennis Science & Technology (2000)
- [4] Mehta, R. Pallis, J. Sports Engineering. **4**, 177-189, (2001)

13.3 Dynamics of confined cavitation bubbles, a possible link with mild traumatic brain injuries.

Amauger Juliette, Guillet T., Decq P., Quéré D., Clanet C. & Cohen C.

LadHyX

juliette.amauger@ladhyx.polytechnique.fr

Traumatic Brain Injury (TBI) is a major healthcare problem, increasingly occurring in sports like rugby, boxing or football. The occurrence of TBI is dependent on the head acceleration and the duration of the shock, as expressed by the empirical Wayne State Tolerance Curve (WSTC). One of the possible causes of TBI is the formation of cavitation bubbles in the cerebro-spinal fluid (CSF). To investigate the link between TBI and cavitation bubbles, we built a model experiment to induce cavitation bubbles through an impact. A tank is entirely filled with water (representing the CSF) and hermetically closed with a flexible membrane (mimicking the CSF circulation between the head and the spinal cord [1, 2]). The tank is impacted on a damper, and the formation and dynamics of cavitation bubbles is observed and studied. After showing that the damaging capacities of such bubbles are in good agreement with the WSTC, we sought to study the influence of the brain: the CSF does not fill the whole cranial cavity, but is confined between the skull and the brain on a thickness of approximately 1mm.

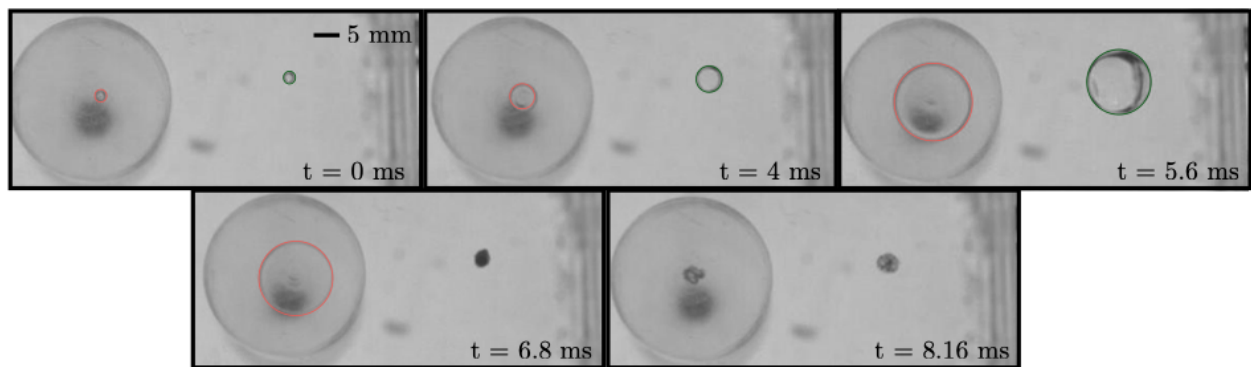


Figure 29: *Chronophotographie de la croissance de deux bulles de cavitation : à gauche (en rouge) une bulle confinée, à droite (en vert) une bulle libre.*

We introduced a confined area in the head-like water tank that allows us to compare the dynamics of confined and unconfined bubbles for the same shock (figure 29). Modeling those confined cavitation bubbles induced by a shock allows us to compute their damaging capacities and conclude on the dangerousness of shocks received by athletes.

References

- [1] C J Avezaat, J H Van Eijndhoven, and D J Wyper. Cerebrospinal fluid pulse pressure and intracranial volume-pressure relationships. *Journal of Neurology, Neurosurgery and Psychiatry*, **42(8)**, 687–700 (1979)
- [2] Mårten Unnerbäck, Johnny T Ottesen, and Peter Reinstrup. ICP curve morphology and intracranial flow-volume changes : a simultaneous ICP and cine phase contrast MRI study in humans. *Acta neurochirurgica*, **160(2)**, 219–224 (2018)

13.4 How Ball Wear Affects Ball Aerodynamics: Do Past Methods Provide an Accurate Representation?

Marriott Hunter, Capel-Davies, J. & Choppin, S.

Sports Engineering Research Group, Sheffield Hallam University

hunter.b.marriott@student.shu.ac.uk

Numerous studies have investigated the effects of wear on tennis ball aerodynamics, predominantly through the use of wind tunnels. Wear has typically been simulated through abrasion and shaving of the felt [1], while tournament-used balls have not been widely tested [2].

In International Tennis Federation (ITF) tournament play, balls are changed out for a new set of six, every nine games. The current consensus is that due to wearing of the felt, "used" balls (9 games) have reduced aerodynamic drag compared to "new" balls [3]. Choppin et al. investigated drag coefficients (C_D) of new and used balls using data from the Hawk-Eye Electronic Line-Calling System for the Davis Cup Tournament (2012 to 2017) [4]. They found that new balls had reduced drag compared to old balls - the opposite of current consensus. It was hypothesized that shaving the felt was an extreme representation of wear, and does not reflect the wear rate after 9 games. This study will evaluate drag of various artificial ball wear methods against new and tournament-used balls to determine their accuracy.

New and used Babolat Team tennis balls were collected from the 2020-2021 Billie Jean King Cup Tournament for wind tunnel testing. Four different wear conditions were tested: new, used, and two artificially worn conditions. Wear was simulated by placing balls in an abrasion box for 2 minutes, and by shaving to remove as much of the nap as possible [2]. Three balls of each condition were tested at wind speeds from 20 to 65 m/s in increments of 2.5 m/s, using a sampling rate of 10 Hz over 10 seconds. Drag coefficient was calculated for each condition.

Wind tunnels tests showed drag coefficients ranging from 0.45 to 0.62, dependent on wind speed and wear condition. Results from paired t-tests at each wind speed showed that each wear condition had significantly different C_D values at all tested speeds ($p < 0.05$). The used balls had higher drag coefficients than new, supporting the findings of Choppin et al., while the shaved balls gave a lower C_D than new balls. Balls worn in the abrasion box had a higher C_D than new, however were still lower than used.

These results indicate that the artificial methods of wear do not accurately represent wear induced from tournament play, particularly when shaving the balls. These findings are contrary to the current consensus that used tennis balls have a lower drag coefficient than new tennis balls, however are consistent with aerodynamics principles.

References

- [1] Chadwick, S.G. & Haake, S.J., *Tennis Science and Technology* (2000)
- [2] Mehta, R.D. & Pallis, J.M., *Sports Eng.* **4**, 177–189 (2001)
- [3] Mehta, R., Alam, F & Subic, A., *Sports Technol.* **1**, 7–16 (2008)
- [4] Choppin, S., Albrecht, S., Spurr, J. & Capel-Davies, J., *ISEA 2018 Proceedings* **2**, 265-271 (2018)

14 Session 9: Biomechanics

Wednesday 8 December - 11h30

14.1 Sensitivity of scapulothoracic angle estimates to kinematic model parameters during ball throwing

Blache Yoann¹, Rogowski I.¹, Degot M.¹, Trama R.¹ & Dumas R.²

1. LIBM, Univ Lyon1, Lyon, France ; 2. LBMC, Univ Gustave-Eiffel, Lyon, France

yoann.blache@univ-lyon1.fr

Investigating shoulder kinematics in overhead sports is challenging due to soft tissue artefact and still demands improvement of kinematic models [1,2]. This study aimed to determine the sensitivity of scapulothoracic angle estimates to kinematic model parameters during ball throwing. Nine healthy males performed sub-maximal overarm throw, while their movements were recorded with a 10-camera system. After calibrating a nominal kinematic model to each participant, fifteen parameters of the nominal models relative to the clavicle length, ellipsoid, sternoclavicular and acromioclavicular joint centers, and contact point location were altered from - 1 cm to 1 cm. Scapulothoracic angles were computed for nominal and altered models using multibody kinematic optimizations. When altering the 15 parameters of the kinematic model, scapulothoracic angles varied up to 49°. Regardless of the degree of freedom, the clavicle length significantly explained the largest part of scapulothoracic angle variance ($16.7\% \pm 3.9\%$, $p < 0.01$). Our study evidences that further research should be conducted on clavicle length estimation when defining shoulder kinematic models in order to use such model to optimize sport performance.

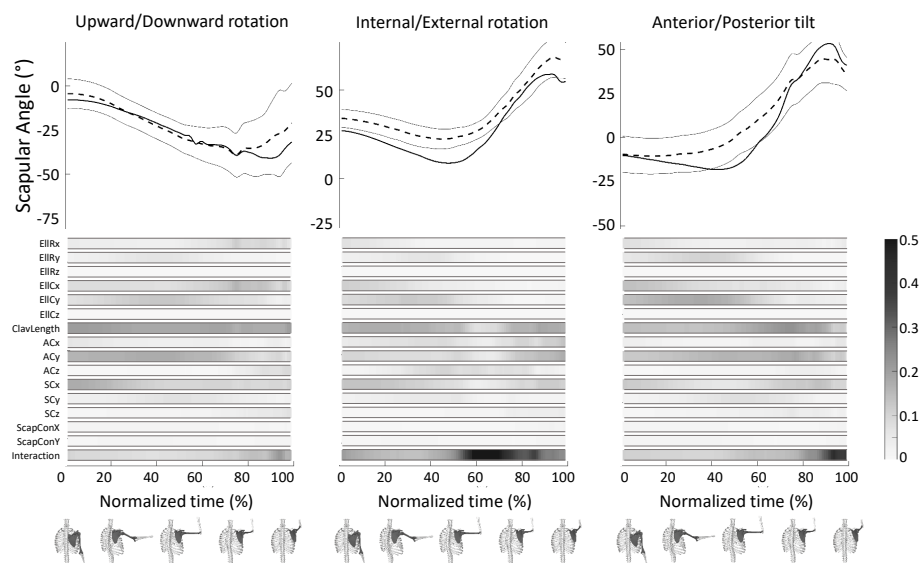


Figure 30: Nominal (thick black line), mean (dashed line), and ± 2 standard deviations from the mean (grey lines) scapulothoracic angles as a function of the normalized time. The color bars represent the average proportion of scapulothoracic angle variance explained by each of the 15 parameters of the kinematic model. *EllR* for ellipsoid radii, *EllC* for ellipsoid center, *ClavLength* for clavicle length, *AC* for acromioclavicular joint location, *SC* for sternoclavicular joint location, *ScapCon* for scapulothoracic contact point location.

References

- [1] Blache Y., Dumas R., Lundberg A. & Begon, M., J Biomech. **62**, 39-46 (2017)
- [2] Begon M., Andersen M.S. & Dumas R., J Biomech Eng. **140**, 030801 (2018)

14.2 Protocol for the mechanical characterisation of a tibial prosthesis: sensitivity study

Doyen Élodie, Szmytka F. & Semblat J.F.

IMSIA, UMR CNRS-EDF-CEA-ENSTA Paris – Palaiseau

elodie.doyen@ensta-paris.fr

This work aims to better understand the dynamic behaviour of the tibial prosthesis to improve long jump performance for tibial amputees while limiting the risk of injury [1]. For that purpose, we intend to optimise its interaction with the track. More specifically, the study will focus on understanding the prosthesis behaviour and the role of the extra sole that is a piece of viscoelastic material added between the extremity of the blade and the sole (see fig. 31).

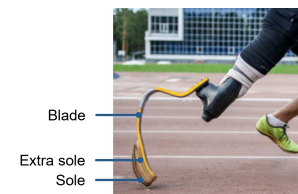


Figure 31: *Tibial prosthesis*

An experimental protocol has thus been proposed based on [2]. The set-up aims to reproduce the step of an amputee athlete at low speed (1 mm/s) on a testing machine. A parametric study is carried out including different parameters: the sole type, the material of extra sole, the shape of extra sole, the ground surface, the angle between the axis of effort and the ground and the alignment of the prosthesis in relation to the axis of effort.

The interaction between the ground surface and the sole is filmed, the strains in the sole and the extra sole are then processed by image correlation (see fig. 32), the effective stiffness and hysteresis of the blade is computed (see fig. 33).



Figure 32: *Strains in standard sole*

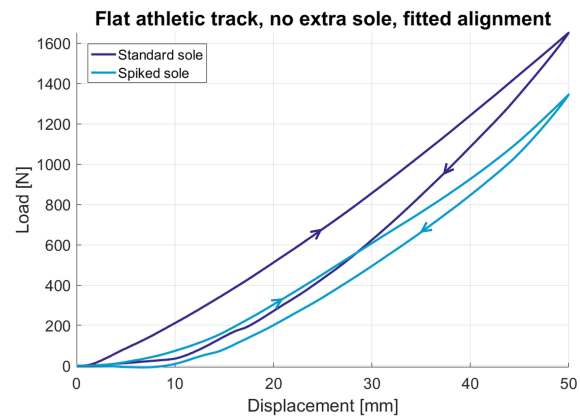


Figure 33: *Force/displacement data*

The effective stiffness depends strongly on the sole used and the geometrical settings. The maximum strain is located at the contact point between the prosthesis and the ground and moves during the step. This experimental protocol enables us to optimise material and geometry of extra sole for better performance.

References

- [1] Doyen E., Canterel N., Szmytka F. & Semblat J.F., ‘Comportement Dynamique d’une Prothèse Tibiale pour le Saut en Longueur’, ENS Rennes - online conference (2021)
- [2] Beck O., Taboga P. & Grabowski A., ‘Characterizing the Mechanical Properties of Running-Specific Prostheses’, PLOS ONE, **11**, no. 12 (2016)

14.3 Force production capacities in sprint running: Citius or Fortius ?

Samozino Pierre, Peyrot N., Edouard P., Nagahara R., Jimenez-Reyes P., Vanwanseele B. & Morin J.B.

Laboratoire Interuniversitaire de Biologie de la Motricité, Université Savoie Mont Blanc : EA7424

pierre.samozino@univ-smb.fr

Sprint acceleration performance depends on the force production capacities in the horizontal direction, the latter decreasing linearly when running velocity increases in human [1]. The aim was to determine the influence of the mechanical Force-velocity ($F - v$) profile (i.e. slope of the $F - v$ relationship) on sprint acceleration performance, independently from the effect of maximal power output associated to horizontal force (P_{Hmax}). A biomechanical model using an inverse dynamics approach applied to the athlete's centre of mass during running acceleration was developed to express the time to cover a given distance as a mathematical function of P_{Hmax} and $F - v$ profile. The model showed very high concurrent validity in comparison to reference measurements (random error $< 4\%$). Simulations showed that sprint acceleration performance depends mainly on P_{Hmax} , but also on the $F - v$ profile, with the existence of an individual optimal $F - v$ profile corresponding to the best balance between force production capacities at low and high velocities (figure 34). This individual optimal profile depends on P_{Hmax} and sprint distance: the lower the sprint distance, the more the optimal $F - v$ profile is oriented to force capabilities and vice versa. When applying this model to the data of 231 male and female athletes from very different sports, force-velocity imbalances (i.e. difference between optimal and actual $F - v$ profile) exist but depend more on sprint distance than on individual $F - v$ profile. Sprint acceleration performance is determined by both maximization of the horizontal power output capabilities and the optimization of the $F - v$ mechanical profile of sprint propulsion.

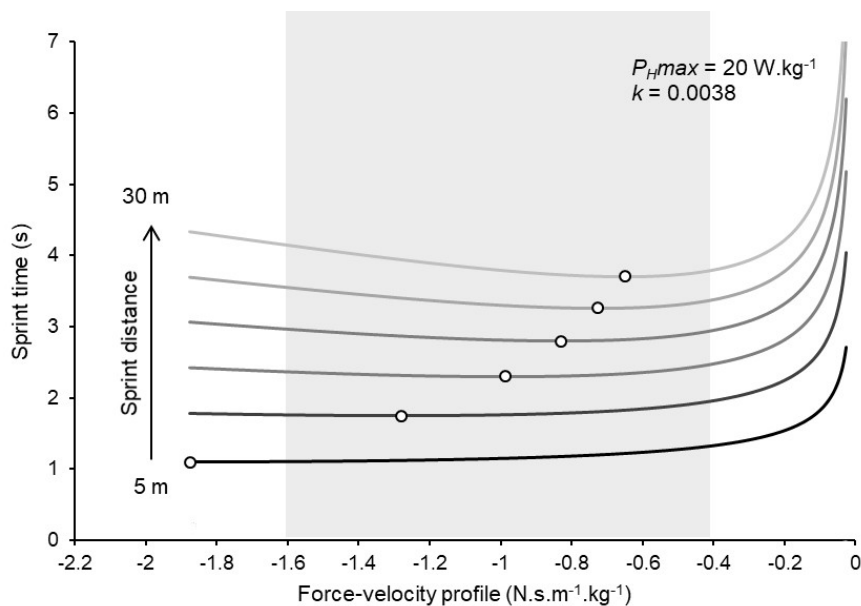


Figure 34: Changes in sprint acceleration time as function of Force-velocity profile for different sprint distances (5, 10, 15, 20, 25 and 30 m) and a given maximal power output in the horizontal direction ($P_{Hmax} = 20 \text{ W.kg}^{-1}$). The grey area represents commonly sprinting $F - v$ profile values previously reported in sport and sciences. The white dots represent the best performances reached at the optimal force-velocity profile for each simulated condition.

References

- [1] Morin J.B., Bourdin M., Edouard P., Peyrot N., Samozino P., Lacour J.R., Eur J Appl Physiol. **112**, 3921-3930 (2012)

14.4 Flexibility of the motor behaviour in swimming

Seifert Ludovic¹, Carmigniani R.², Guignard B.¹, Letocart A.¹, Simbana D.³

¹CETAPS EA3832, Faculty of Sport Sciences, University of Rouen Normandy, France, ²LHSV, Ecole des Ponts Paris Tech, EDF R & D, France, ³Fédération Française de Natation, France

ludovic.seifert@univ-rouen.fr

Recent research has investigated the flexibility of the motor repertoire of swimmers advocating to a physical law applied to human movement science [1, 2]. On this basis, Carmigniani et al. [1] looked for the inter-limb coordination (assessed by the index of coordination, IdC) that would make possible to minimise the mechanical energy consumption at a given speed. At low speed, the swimmers kept a constant IdC (in catch-up pattern) and varied their speed by increasing their mean propulsive force (Figure 35). When they reached their upper bound of maximal force, the propulsion time was minimal and did not vary. To further increase their speed, the swimmers had to reduce their non-propulsive phases and the time between two propulsive phases.

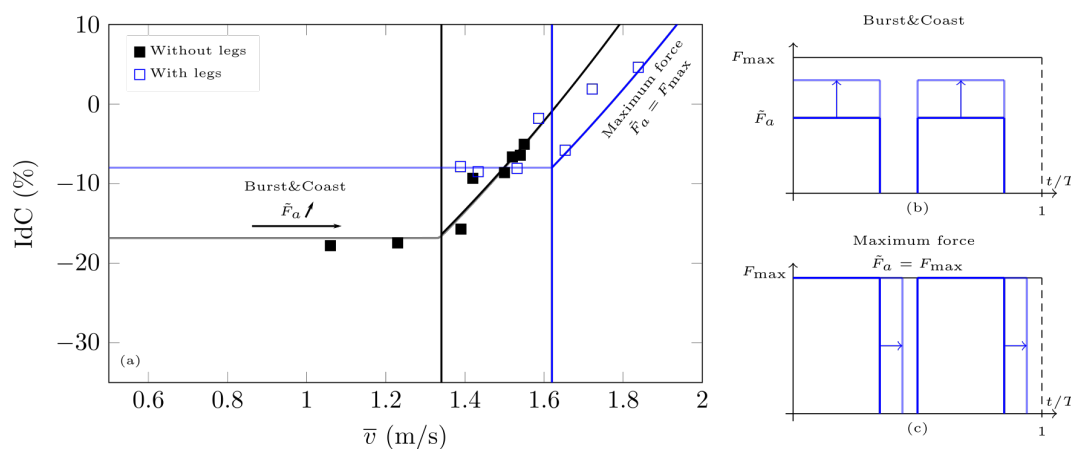


Figure 35: Coordination changes with speed: (a) Evolution of the coordination. (b) The model predicts a low velocity regime of burst-and-coast, and (c) a maximum force regime.

In summary, two regimes appears in front crawl: first, at low speed and low drag, swimmers minimise energy consumption with results in stable stroke length and catch-up pattern of coordination. Second, when speed and drag increase (above a threshold that seems to corresponds to the 200m race pace [3]), swimmers used a maximal force regime characterised by high increase of stroke rate and of the continuity between propulsive actions, which above 1.8 m/s led to a superposition pattern of coordination. Although these two regimes could be identified in the swimmers, inter-individual variability could be observed. Therefore, the current presentation exemplifies some case studies of effective and less effective swimmers, and then provides practical application for training.

This work was funded by the ANR NePTUNE (ANR-19-STHP-0004).

References

- [1] Carmigniani, R., Seifert, L., Chollet, D., Clanet, C., *Coordination changes in front-crawl swimming*. RSPA, 476(2237),2020
- [2] Chung, M.H., *On burst-and-coast swimming performance in fish-like locomotion*. Bioinspiration and Biomimetics. 4(3), 2009
- [3] Seifert, L., Chollet, D., Rouard, A., *Swimming constraints and arm coordination*. Human Movement Science, 26(1), 2007

14.5 Theoretical framework of a force-velocity-endurance relation

Morel Baptiste¹, Bowen M.¹, Dorel S.² & Samozino P¹.

¹ LIBM - Inter-University Laboratory of Human Movement Biology

² MIP - Movement, Interactions, Performance

baptiste.morel-prieur@univ-smb.fr

Muscles are the actuators that drive human movement. Due to their molecular structure the force production is lower when the shortening velocity is higher [1]. Considering the cycling movement, the mechanical resultant is a torque applied to the bottom bracket (Γ in N·m) for a given angular velocity ($\dot{\theta}$ in rad·s⁻¹); Eq. (1). During maximal intensity exercise, muscle capacity decrease following an exponential decay function, the asymptote being named critical intensity; Eq. (2) [2]. Another way to describe this phenomenon is to consider that the maximal muscle capacity is inversely proportional to the work done above the critical intensity (W_{AC}); Eq. (3). Based on these assumptions we propose to characterize the torque-cadence-endurance capacity following $\Gamma(\dot{\theta}, t)$ and $\Gamma(\dot{\theta}, W_{AC})$ relations (figure 36). This mathematical framework would help to optimize track cycling performance for instance by finding the gear ratio that maximize the total work done during a race.

$$\Gamma = \Gamma_0 \left(1 - \frac{\dot{\theta}}{\dot{\theta}_0} \right) \quad (1)$$

$$\dot{\theta}_0(t) = \dot{\theta}_{0e} + (\dot{\theta}_{0i} - \dot{\theta}_{0e}) e^{-\frac{t}{\tau_{\dot{\theta}_0}}} \quad \wedge \quad \Gamma_0(t) = \Gamma_{0e} + (\Gamma_{0i} - \Gamma_{0e}) e^{-\frac{t}{\tau_{\Gamma_0}}} \quad (2)$$

$$\dot{\theta}_0(W_{AC}) = \dot{\theta}_{0e} + \beta_{\dot{\theta}_0} \times W_{AC} \quad \wedge \quad \Gamma_0(W_{AC}) = \Gamma_{0e} + \beta_{\Gamma_0} \times W_{AC} \quad (3)$$

$$W_{AC}(T) = \int_0^T (P_m(t) - P_C(\dot{\theta})) dt \quad (4)$$

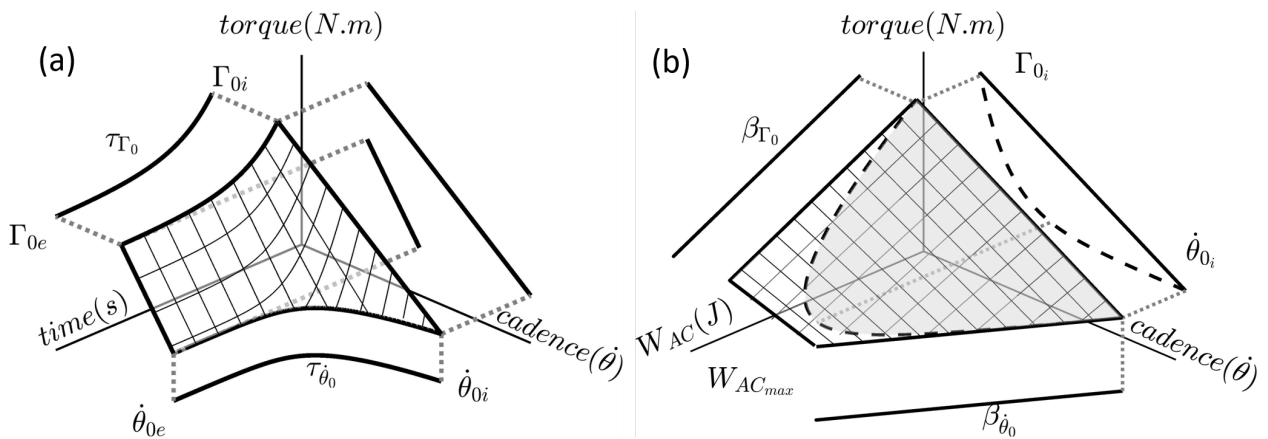


Figure 36: Force-velocity-endurance capacity expressed as (a) $\Gamma(\dot{\theta}, t)$ and (b) $\Gamma(\dot{\theta}, W_{AC})$.

References

- [1] Sugi H.& Ohno T., Int. J. Mol. Sci. **20**(12), 3075 (2019)
- [2] Poole D., Burnley M., Vanhatalo A., Rossiter H. & Jones A., Med. Sci. Sports Exerc. **48** (11), 2320 (2016)

15 Session 10: Material

Wednesday 8 December - 14h00

15.1 Guiding blind people with spatialized sound for sport practice

Ferrand Sylvain, Alouges F., Aussal M.

Centre de Mathématiques Appliquées, Ecole Polytechnique, CNRS, IP Paris

sylvain.ferrand@polytechnique.edu

Everyone is able to locate and track a sound source and this is especially true for blind people that use this ability in everyday life. They are using it, for exemple to follow the steps of the person in front of them on the street or in sports practice to follow a guide when running or roller blading.

Using the same principle, it seems possible to guide people with spatialized sounds generated in real-time and listened with simple headphones (binaural listening). Indeed, if we can localize the person precisely in real-time, it is possible to create a virtual sound source ahead of him/her that guide him/her along a pre-defined path. We have therefore explored this methodology and developed an autonomous embedded device capable of guiding people using *binaural synthesis*. This device is particularly suitable to the practice of sports in well controlled environment.

Binaural sound synthesis seeks to reproduce the properties of natural listening by digital filtering. The basic principle consists in using audio cues named Interaural time differences (ITD), interaural level differences (ILD) and spectral information due to reflexions and diffractions by the head and the body of the listener. Those are summarized in filters called Head Related Transfert Functions (HRTF).

The talk proposes to make and overview of these techniques together with a clear description of the device [1] that was built. It includes in particular an accurate positioning GNSS type system and an IMU in order to monitor the orientation of the head. Results in real environments, including figure 37, will be presented showing the reliability of the approach. We have thus been able to confirm that spatialized sound could constitute an effective tool for guiding blind people, without inducing any penalizing cognitive load, for practicing sports such as walking, running or rollerblading in partial autonomy, including the context of performance.

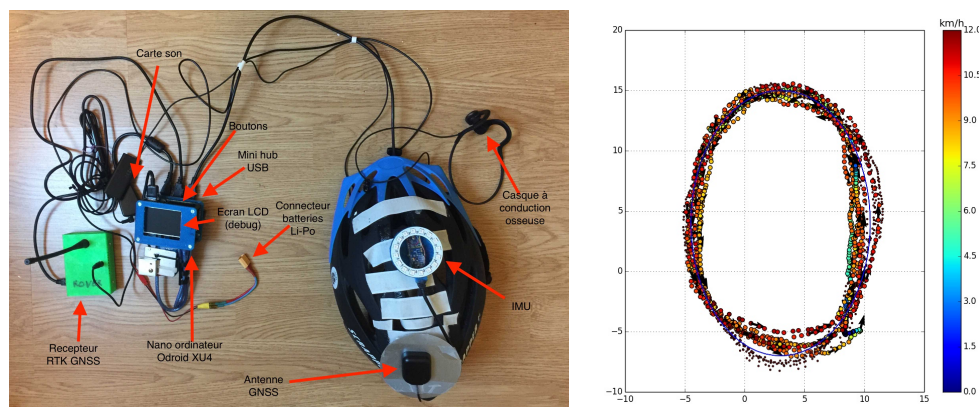


Figure 37: Left : the complete device, including a computing unit, a GNSS, a head tracker and a bone conduction headset. Right : Course of a blind roller-skater (Stephane Le Sueur, MCV), several turns along an elliptical track.

References

- [1] S. Ferrand & F. Alouges & M. Aussal, "An electronic travel aid device to help blind people playing sport," in IEEE Instrumentation & Measurement Magazine, vol. 23, no. 4, pp. 14-21, 2020

15.2 Optimizing shoe midsoles for running performance

Fay Sarah C. & Hosoi A.E.

Mechanical Engineering, Massachusetts Institute of Technology

scfay@mit.edu

Additive manufacturing has become a viable and trendy production method for the cushion-providing parts (the midsoles) of running shoes. Such a 3D printed midsole is shown in the figure below. While traditional midsoles are made from a uniform foam material, shoes made with 3D printing technology can be designed to have mechanical properties which vary at different locations under the runner's foot. This expansion of the design space should therefore allow for the creation of higher performing running shoes than those with traditional properties. However, exploring the design space is difficult because fabricating and testing new designs is a slow and expensive process. To identify shoe designs that may be high-performing (and worth testing in a lengthy experiment), a method for predicting the performance of midsole designs was developed and tested.



Figure 38: *Running shoe created to have model-predicted optimal stiffness properties in its 3D printed midsole.*

The proposed method is both data-informed and based in physics. The underlying model for running is based on simple mechanical elements (actuators, springs, and dampers) and is an expansion on the model used to determine the optimal track stiffness (used to create the high-performing Harvard indoor track [1]). The new model successfully recreates the relationship between shoe properties and running performance for well-established shoe designs, and it allows the flexibility for evaluation of shoes which have yet to be made, particularly those in the new design space afforded by the advances in additive manufacturing. Specific lattice-structured midsole geometries, were then evaluated using this method, and the predicted highest performing shoe design was fabricated (shown in the figure) for further evaluation.

References

- [1] McMahon T.A. & Greene P.R., *J. Biomech.* **12.12**, 893–904 (1979)

15.3 Modeling of additive manufactured lattice structures designed for shock-absorbing sports components

Hassaine-Daouadji Valentin, Carreira R.P., Witz J.F. & Brieu M.

DECATHLON Technical Office, DECATHLON SA, Lille, France

valentin.hassaine@decathlon.com

Additive manufacturing enables the production of complex parts such as lattice structures. Their potential, in terms of lightness, improved impact performances, customization and design, draws the attention of the sports equipment manufacturer *DECATHLON*, who is considering these meso-structures for helmets and shoes applications. This study goes from the analysis of lattice materials to the understanding of the behaviour of structures under compressive loading. This multi-scale approach is presented in *the figure*.

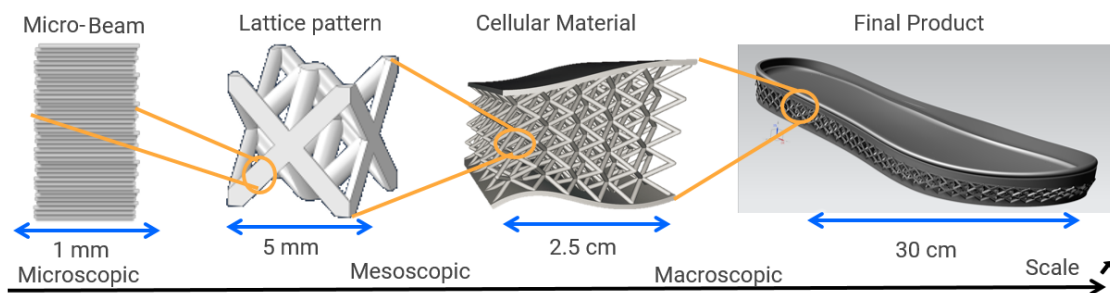


Figure 39: *Multi-scale approach*

A preliminary experimental phase identified the behaviour of two materials (PA12 and TPU) produced by a laser sintering process (SLS). The technical feasibility of lattices structures in sports products was then evaluated using static compressions compared to traditional helmet and footwear foams.

The second stage of the study consists in developing numerical tools for the design of lattices structures. Several lattices were analysed in detail under compressive loadings. In addition to the static response, the dimensional stability of the structures and the quantification of the kinematic fields under stress were assessed by micro-tomography.

Thanks to these observations, the relevance of a numerical lattice model realized under a finite element code was evaluated. Its lack of representativeness of the junction zones of the beams (the vertices) limits its use. Nevertheless, a local stiffening at the vertices, studied by a numerical design of experiment, greatly improved the modeling.

References

- [1] Hassaine-Daouadji V., Carreira R.-P., Witz J.-F. & Brieu M., *Advanced Structured Materials* **132**, 305–322 (2020)

16 **Keynote 6: Two short stories about data and sports**

Wednesday 8 December - 14h50

Hosoi Anette

MIT Sports Lab, USA

peko41@gmail.com

Recent advances in data collection, make sports an ideal testing ground for new analyses and algorithms. In this talk I will describe two studies that lie at the intersection of sports and data.

In most professional sports, every physical attribute of an athlete that can be measured is quantified and used to estimate athletic potential. However, coaches know that physical ability is only one piece of the puzzle; cognitive aspects of the game, including the ability to make sound decisions under pressure, play an important role in athletic success. In most games, these decisions manifest as physical actions that can be captured in tracking data. Here I will describe a framework for evaluating decision-making, while simultaneously making inferences around game strategy and execution efficacy. The framework is built on an Expected Possession Value (EPV) metric in basketball that is computed through tracking data that is then leveraged to identify scoring opportunities throughout a game. We analyze these opportunities as instances of decision-making and quantify the quality of these opportunities and how often they are missed. Looking at team opportunities as a whole and relying on the notion of expectation, we are able to determine how much of a team's performance can be attributed to their strategy versus their execution.

The second story explores the impact of opening NFL stadiums to fans during the pandemic. During the 2020-2021 season, each NFL team put forward their own plans and negotiated with the league, the relevant state, and their local community to determine whether they would be able to open the stadium to fans. Borrowing techniques from economics, we apply synthetic control methods to analyze covid case counts to determine whether opening stadiums has a detrimental, beneficial or neutral effect on the surrounding community.

Alphabetical index of authors

- Abel, 19
 Alouges, 46
 Amauger, 39
 Aniszewska-Stepień, 34
 Antony, 9
 Audot, 13
 Augier, 32
 Aussal, 46

 Bailly, 12
 Banhegyi, 33
 Banks, 13
 Bazuin, 21
 Begon, 12
 Belhadji, 28
 Bendimerad, 27
 Benham, 10, 27
 Benzaquen, 27
 Bergeron, 16
 Best, 8
 Bideau, 7
 Blache, 41
 Blanchard, 22
 Bocquet, 18
 Boillet, 14
 Bolon, 30
 Bot, 32, 37
 Bou Saïd, 24
 Boucher, 5, 11, 25
 Boulanger, 31
 Bowen, 45
 Brieu, 48
 Brisard, 23
 Brunet, 4, 19, 20, 25

 Capel-Davies, 38, 40
 Carmigniani, 11, 18, 23, 26, 28, 30, 44
 Carreira, 48
 Cavoret, 8
 Charbonneau, 12
 Choppin, 38, 40
 Cintrat, 37
 Clanet, 11, 14, 18–20, 22, 23, 25–28, 30, 39
 Cohen, 14, 17–20, 22, 26, 39
 Colard, 14
 Comtet, 25

 de la Hougue, 32
 Decq, 39
 Deggot, 41
 Demestre, 7
 Devauchelle, 10
 di Prampero, 15
 Diry, 14

 Dode, 14, 18
 Dolique, 9
 Dorel, 45
 Douin, 37
 Doyen, 42
 Dumas, 41
 Dumont, 7
 Dureisseix, 24

 Edouard, 43

 Farnesi, 37
 Fauchoux, 17
 Fay, 47
 Ferrand, 17, 46

 Géminard, 6, 9
 Gasso, 34
 Gorgels, 33
 Grange, 7
 Grasso, 19
 Guignard, 31, 44
 Guilbert, 8
 Guillet, 39

 Hérault, 34
 Hacques, 34
 Hasbroucq, 11
 Hassaine-Daouadji, 48
 Homo, 23
 Hosoi, 47, 49
 Hudson, 13

 Iachkine, 32

 Jimenez-Reyes, 43
 Jux, 21

 Karamanoukian, 5

 Labbé, 5, 11, 25
 Lallemand, 22
 Lanaspèze, 8
 Lanos, 37
 Larrarte, 30
 Le Cunuder, 29
 Le Vergos, 32
 LeFranc, 17
 Letocart, 31, 44
 Lustig, 23

 Maciejewski, 14
 Maddalena, 17
 Manin, 8, 9
 Marimon Giovannetti, 33
 Marriott, 38, 40
 Messonnier, 14

 Milani, 17
 Mille, 6, 29
 Morel, 45
 Morin, 43
 Morio, 36
 Morris, 10

 Nagahara, 43
 Neufeld, 10
 Nicolas, 7

 Odier, 29

 Péraud, 25
 Papola, 37
 Pernod, 32
 Peyrot, 43
 Pezzoli, 33
 Plougouven, 20
 Pontonier, 7
 Prétot, 11, 26, 28, 30

 Quéré, 39

 Rémond, 9
 Ramirez, 37
 Rinaldi, 9
 Robert, 19
 Rogowski, 41
 Rouillon, 22
 Roy, 20

 Sacher, 32
 Samozino, 43, 45
 Sciacchitano, 21
 Seifert, 31, 34, 44
 Semblat, 42
 Simbaña-Escobar, 31
 Simbana, 44
 Szymtka, 42

 Thomson, 13
 Trama, 41

 van de Water, 21
 van den Berg, 21
 Vanwanseele, 43
 Vedel, 24
 Vignais, 5
 Ville, 8
 Vincent, 22
 Violeau, 26

 Warner, 13
 Westerweel, 21, 35
 Witz, 48

Acknowledgements

The organising team of the conference wants to thank the Laboratoire de Physique, ENS de Lyon, CNRS and the Metropole de Lyon for their financial support to the conference. They also want to thank the initiative *Science*²⁰²⁴ for their active support in relaying the informations about the conference and participating to its scientific organisation.

